Russian Geology and Geophysics
Vol. 41, No. 1, pp. 1-29, 2000

Geologiya i Geofizika
UDC 551.24+551.1312.4+551.33

LATE CENOZOIC PALEOCLIMATE RECORD IN BOTTOM SEDIMENTS OF LAKE BAIKAL (*600 m deep drilling data*)

Baikal Drilling Project Group*

One more drilling experiment, as part of the Baikal Drilling Project, was carried out in 1998 on the Akademichesky Ridge. Drilling was performed to the subbottom depth of 670 m in 333 m of water at 53°44′48′′ N, 108°24′34′′ E. Continuous coring was completed to 600 m with a core recovery of 95%. The BDP-98 section is composed of alternating biogenic (diatom-bearing) and terrigenous (diatom-barren) muds. This rhythmic structure traceable along the entire core formed in response to alternating cold and warm climates. Variations in diatom abundance correlate with biogenic silica, magnetic susceptibility, water content, and density profiles. Proceeding from paleomagnetic studies and analysis of the Earth's orbital frequencies in the climatic record of the core, the sediments at a depth of 600 m were dated at 10.3 Ma BP. The results of core studies provide a basis for further detailed climate reconstructions in Central Asia from the late Middle Miocene and make it possible to refine the geological history of the Baikal rift.

Drilling, lithology, sedimentation, muds, diatoms, seismic section, logging, radioactivity, thermal conductivity,core,paleomagnetism

INTRODUCTION

One more scientific drilling experiment was carried out on the Akademichesky Ridge by the international team of the Baikal Drilling Project in 1998. During the first drilling there, in 1996, two boreholes were drilled to total subbottom depths of 100 and 300 m; the latter hole was cored to 200 m [1]. The two holes, as well as the boreholes in the Bugul'deika Saddle [2], were drilled by the Nedra-Baikal-600 drilling complex deployed on a 400 ton ice-based barge capable of working at a water depth of 400 m. In the summer of 1997, an enhanced drilling system Nedra-Baikal-2000 was mounted on a 1300 ton barge to reach 1 km drilling depth in up to 900 m of water. The drilling experiment of 1997 was carried out in the South Baikal basin, where the lake is 1428 m deep [3].

The 200 m long BDP-96 sedimentary core, retrieved during the drilling experiment of 1996, spans 5 Ma, and the vertical profiles of diatoms and biogenic silica in it correlate well with the marine oxygen isotope curve [4]. In the following experiment it was projected to drill at 53°44′48′′ N, 108°24′34′′ E in 333 m of water. The selection of site was determined by a greater thickness of the middle section, which suggested higher sedimentation rates than those in the 1996 section. Another reason was that the site was away from large faults and coarse deltaic deposits revealed in seismic profiles in the southeastern part of the ridge. The barge was trailed by the support ship *Baikal*, more powerful than the previously used one.

The field trip started on 27 December 1997. On 7 January 1998, the remainder part of the team was picked up aboard at the exit from Maloe More in Zama Bay. On 8 January, the complex took a start to the drilling site and was finally fixed at the drilling point on 14 January. The first core was recovered on 18 January. The experiment completed on 5 April, and on 5 May 1998, the complex safely returned to port Baikal.

* V. Antipin, T. Afonina, O. Badalov, E. Bezrukova, A. Bukharov, V. Bychinskii, D. Williams (USA), A. Gvozdkov, V. Geletii, V. Golubev, A. Goreglyad, I. Gorokhov, A. Dmitriev, R. Dorofeeva, A. Duchkov, O. Esipko, E. Ivanov, N. Yoshida (Japan), T. Kawai (Japan), I. Kalashnikova, G. Kalmychkov, E. Karabanov, E. Kerber, J. King (USA), K. Konstantinov, V. Kochukov, V. Kravchinskii, M. Krainov, L. Kukhar', N. Kudryashov, M. Kuz'min, K. Nakamura (Japan), S. Nomura (Japan), E. Oxenoid, L. Pevsner, J. Peck (USA), A. Prokopenko, V. Romashov, H. Sakai (Japan), I. Sandimirov, A. Sapozhnikov, K. Seminskii, N. Soshina, L. Tkachenko, M. Ushakovskaya, T. Fileva, B. Khakhaev, O. Khlystov, M. Khuzin, and G. Hursevich

This paper summarizes preliminary results of BDP-98 core studies.

GEOLOGICBACKGROUND

The borehole BDP-98 was drilled on the Akademichesky Ridge (Fig. 1), a submerged asymmetrical horst bounded by the Ushkan'yi fault in the northwest and by the Ol'khon fault in the southeast, which separates the Northern and Central subbasins of Lake Baikal. The ridge rises for 500 m above the lake bottom in the northwest and is as high as over 1000 m in the southeast, with 300 to 350 m average water depth over its top. The basement surface is overlain by 1000–1500 m thick sediments, thinning down to a few meters on the southwestern (Ol'khon Island) and northeastern (Ushkan'yi Isles) extremities of the ridge. Bedrocks are exposed on the ridge sides.

The seismic stratigraphy of the sedimentary section has been fairly well studied and described in a number of papers [5–8]. Multichannel seismic profiling revealed two major seismic units in the section (Fig. 2). The <200 m thick thinly stratified upper unit (A) deposited during the Angarian stage (named after the Upper Angara River) of the Baikal evolution [8], and the lower unit (B), over 1000 m thick, formed during the Barguzin stage. The two seismic units are separated by an erosional unconformity expressed as an acoustic boundary B10. The lower unit includes two subunits: The upper finely laminated one (B10–B6) deposited in relatively steady limnic conditions, whereas the lower unit (B6–B5) contains wedge-like features indicating deposition in the Paleo-Barguzin delta. According to the seismic pattern, the sediment transport was from east to west [8]. The deltaic deposits give way northwestward to a layered sequence produced by finer-grained sediment load transported off the delta from the paleoriver.

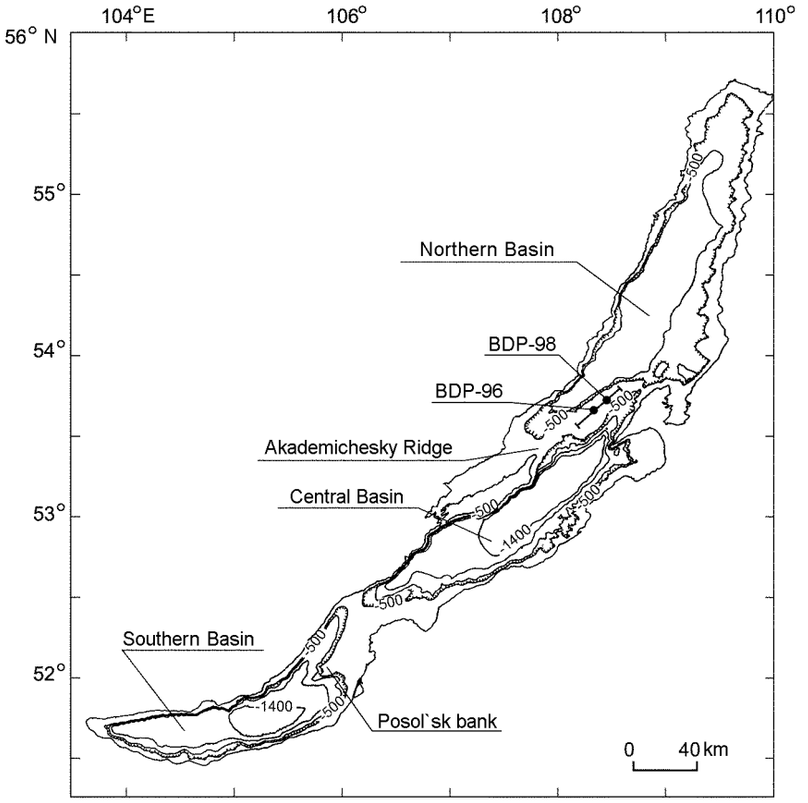

Fig. 1. Bathymetric map of Lake Baikal and BDP-96 and BDP-98 core site locations on Akademichesky Ridge. Solid line is a segment of CDP seismic reflection profile 92-15 shown in Fig. 2.

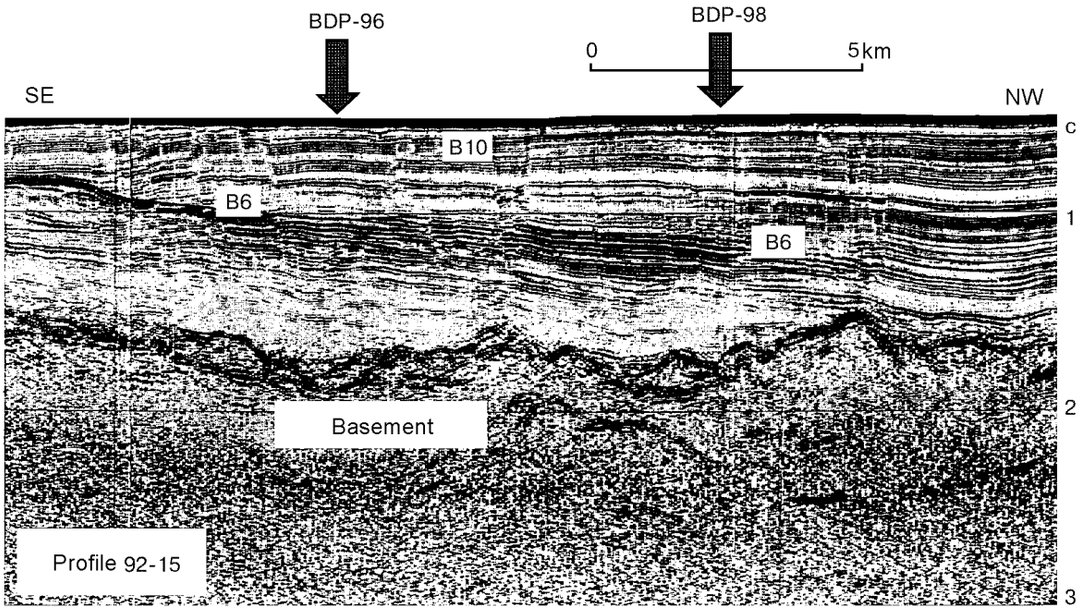

Fig. 2. Seismic profile 92-15 along the top of Akademichesky Ridge, after [6]. Principle seismic boundaries B6 and B10, after [8]. Arrows point to core sites. Seismic unit A is above acoustic boundary B10.

The lowermost part of the unit (B4–B1) is composed of deformed sediments which yield a discontinuous acoustic pattern. The sediments fill lows of the basement surface or, occasionally, cover the slopes of these lows and lay upon the basement with angular unconformities. According to preliminary estimates [8], the onset of the Angarian stage, marked by the erosional boundary B10, corresponds to the Lower/Upper Pliocene boundary (ca. 3.5 Ma), and the boundary B10 itself corresponds to the Early Pleistocene [7] neo-Baikalian stage of rifting.

This boundary was expected to have been stripped by BDP-96, as the sediments at the end of the section are about 5 Ma old, but the core showed no evidence of erosion. Moreover, the 1996 drilling experiment confirmed that deep-water limnic sedimentation on the eastern flank of the Akademichesky Ridge continued through the past 5 Ma.

Analysis of the BDP-96 core revealed a constant and continuous sedimentation rate of 4 cm/1000 years over the past 5 Ma. If the BDP-98 sediments deposited at the same rate, the end of the section should be at the 14/15 Ma boundary (Middle Miocene) and pass the acoustic boundary B6. Middle-Upper Miocene deposits on Ol'khon [9, 10] belong to the Tagai Formation overlain by the Upper Miocene-Lower Pleistocene Sasa Formation.

Early Miocene climate in the south of Siberia, as inferred from studies of sedimentary sections on Ol'khon and in southern Siberia [11, 12], was similar to that of southern subtropics (e.g., present-day Transcaucasia [11]), with a mean January temperature above zero and a mean June temperature of 28 °C; mean annual precipitation was 1500 mm.

The Middle Miocene climate was colder and drier, with a mean January temperature of 0 to –6 °C and summer temperatures nearly the same as in the Early Miocene. The Middle Miocene flora of southern Siberia may have been similar to that of the modern forests in southern China at 35–42° N [11].

The Late Miocene climate was still colder and less humid, with the average winter temperatures decreased down to –10 °C and precipitation reduced to 1000 mm/year. These changes led to extinction of many thermophile and hydrophile plants, such as magnolia, tulip tree, chestnut, marsh cypres, beech, etc. [11].

The Early Pliocene climate was quite warm and moderately humid but became colder and more continental by the end of the Pliocene. The January temperatures fell to –15, –20 °C, and precipitation was as low as 300–400 mm/year.

Since the second half of the Late Pliocene, the climate progressively grew colder and moister [11] till the

stage of severe cooling, which set in the early Quaternary and was then repeatedly broken by relatively warm interstadials [11, 12].

RESULTS OF DRILLING AND CORE STUDIES

Drilling technology, core recovery, and correlation of cross sections

The borehole BDP-98 was drilled by a Nedra-Baikal-2000 drilling complex deployed on a 1300 ton barge. The complex comprised a drill, a drilling rig, drilling pumps, a set of power stations, and a flushing system. The drill column was fabricated using light-alloy 147× 11 tubes.

During the experiment, three holes were drilled. One penetrated 201 m of sediments and was drilled using a drilling column, without a raiser. The second hole was drilled, for the first time on Baikal, with the use of a 245 mm long raiser fixed at a subbottom depth of 180 m, which allowed the drill to move up and down without missing the hole and to flush the borehole with a mud solution circulating in the closed system collar—face—collar. This made the hole walls more stable and facilitated slam removal. As a result, a section 674 m thick was successfully drilled and cored continuously to a depth of 600 m. The third hole reached a depth of 100 m, and six cores were sampled in order to compensate for the loss in the first hole.

To obtain a continuous 600 m thick section, the second hole was cored from a subbottom depth of 191 m to have a 10 m overlap with the first hole. The two holes showed a good core-to-core correlation, observed in laboratory from comparison of biogenic silica profiles; the second hole was shifted 30.5 cm upward relative to the first one, which was taken into account when the two sections were joined into a composite record.

Continuous cores were obtained using a corer Baikal-2 and a new universal Baikal-Global corer (which was designed at the Nedra Designing Center in cooperation with the Drilling Technology Institute and was used for test during the 1998 experiment) equipped with removable corers for various recovery methods. Most of the coring was done with the Baikal-2 corer, which proved efficient in the drilling experiments of 1993 and 1996 [1, 2]. During the 1998 experiment, the core was recovered with an advanced hydraulic piston corer (APC) to a subbottom depth of 270 m, and rotary drilling was used to complete the coring. The total core recovery was over 95%, up to 98% at some intervals.

Special measures were taken to avoid surficial sediment loss. The piston corer made a number of test shots as the drill was slowly submerged after the water depth at the drilling point was measured by a log winch and surficial sediment was cored by the piston. In the recovered uppermost section there is a boundary between the upper oxidized and the lower reduced sediments. The oxidized upper layer is 11 cm thick and contains a ferromanganese crust, typical of the Akademichesky Ridge, i.e., an undisturbed sediment surface was recovered.

The experiment included measurements of water content and density of sediments, preliminary lithological description of the core, and repeated sampling of released gas. Geophysical logging was carried out during and after the drilling.

Lithology of the BDP-98 section

The sedimentary section of BDP-98 (Fig. 3) is composed of fine pelitic-silty biogenic and terrigenous muds, with a denser and more silty lower part of the section. The diatom abundances — diatom frustules counted in smear slides (Fig. 3) — vary from 0 to 90% and show pronounced alternation of clays and diatom-rich sediments throughout the section. The abundance of diatom frustules increases notably between 100 and 370 m, where it is at least 10–15%, and the upper 100 m and the lower 490-600 m of the section are virtually barren of diatoms (less than 5%).

The diatom record (Fig. 4, *a*) can be divided into several intervals in which average abundances of diatoms and their variation patterns are relatively uniform: 0–110; 110–270; 270–480, and 480–600 m. In the first interval, diatoms show a low average content with variations from 0 to 65% and a high periodicity of the signal. The average diatom content is higher in the second interval (about 25%), which shifts the record to the right relative to the first interval. In the other intervals, the diatom abundances are lower; the signal in the last interval shows wide peaks, and the minimum decreases to 5%.

Figure 4, *b*, *c* shows variations in percentages of pelitic and silt-sand particles. The pelitic fraction is most abundant from 0 to 120 m and decreases to 10% from 120 to 130 m, at the account of a greater abundance of diatoms. The percentage of clay-size particles is nearly constant from 130 m up to the end of the section but is much lower than in the upper 120 m. In the interval from 130 to 270 m, the percentages of pelitic

particles are more variable than those in the lower part of the section (270–600 m) in which they are very poorly pronounced except for a few short intervals.

The total content of the sand-silt fraction in the interval of 0 to 160 m fluctuates at a higher rate and amplitude than elsewhere over the section. At a depth of 170–190 m it is very low and then increases slightly from 200 to 600 m. This tendency is best evident in the plot showing percentages of pelitic and sand-silt particles relative to 100% (Fig. 4, *d*). Below 200 m, pelitic particles are much less abundant. In the coarse-grained fraction, silt particles predominate, and the sand fraction does not exceed 5%, increasing to 10–25% in a few layers in the lower section. Sand-silt particles are also present as small lenticular inclusions throughout the section.

The recovered sediment is of gray color, except for the uppermost 11 cm thick oxidized section with a layered structure produced by thinly alternating black to brown and brown to yellow bands. Below there are gray reduced deposits traceable as far as the borehole face. Note that the clay layers are light-colored (grayish) and the diatomaceous layers are darker (olive or green) and darken downcore to olive-black and black, possibly, because of abundant plant remnants and humic substances.

The sediments, as a rule, have laminated, finely laminated, massive, or lenticular structures, with lamination produced primarily by alternating diatom ooze and terrigenous clays. Fine lamination is caused by variations in diatom abundances or by the presence of layers with varying iron and manganese contents related to fluctuations of sedimentation rate [1], which is well evident in the upper 200 m. This type of layering is worse pronounced in the middle section, and lamination of the lower 500 to 600 m is chiefly due to the varying grain-size distribution and the appearance of coarser-grained layers. The thin lamination is best evident in gamma-tomography images (see, for instance, core 5 from a depth of 7–9 m in Fig. 5).

The middle part of the core (depths 125 and 149 m) contains scarce 30–50 cm thick bands with chaotic structures in which the primary layering is disturbed, and the layers are folded and deformed, possibly by microsliding.

Traces of bioturbation are distributed unevenly over the sediments. In the upper 100 m they are few and are best evident in diatom-rich layers as small horizontal lenses of a slightly different color. Bioturbation disturbs the continuity of silt-sand layers and is weakly pronounced in clay layers. It is more intense in the middle section (from 150 to 300 m), where the average diatom abundance is relatively high, and is very weak in the lower section. At the same time, it nowhere leads to complete destruction of layers, which indicates that its role in the deposition on the Akademichesky Ridge was insignificant.

Lenticular structures, not related to bioturbation, are ubiquitous throughout the section and are due to the presence of sand-silt lenses measuring 0.*n* mm to 1 cm. According to their number (Fig. 6, *a*), morphology, position, and roundness, the core can be divided into several segments. The sand-silt lenses are most abundant through the core depth from 0 to 250 m. In the upper 130 m they are, as a rule, elongate, randomly oriented, angular or poorly rounded; their appearance is most likely related to icebergs or ice rafting [1, 13]. Sand lenses at 130 to 300 m are less numerous, better rounded, and apparently were transported by seasonal ice rafting. From 250 to 500 m of core depth, sand lenses are still scarcer. Their amount increases slightly only in the lower 100 m, where they are positioned nearly horizontally and their coarse-grained fraction includes fine gravel and well-rounded sand and gravel particles.

Gravel grains (Fig. 6, *b*) are most abundant in the lower part of the section, especially in the lower 100 m, where their number attains 10 grains per 1 m of core, and they are well rounded. In the upper section, gravel grains are much less numerous and poorly rounded. The upper 100 m section also contains scarce pebbles rarely exceeding 2–3 cm in size (Fig. 6, *b*). One, about 5 cm in diameter (Fig. 7), is a flat and well-rounded pebble of green schist found in a clay layer, with a typical glacial striation. Pebbles of this kind, as well as angular gravel grains from the upper section, make coarse ice-rafted detritus that was delivered to the lake by glaciers and to the sediments of the Akademichesky Ridge by icebergs. Ice rafting may have been also responsible for the presence of small clay fragments (a few centimeters in diameter) mostly in the upper part of the section.

Coarse-grained layers (Fig. 6, *c*) are scarce in the upper section and more numerous below the core depths of 480–490 m. They differ in their position in the section and in internal structure.

The first distinct sand layer is 13 cm thick and occurs at the core depth of 52.37 m, in a clay layer. Its base is uneven, with traces of erosion. The structure is graded, caused by fining of particles — from medium- to fine-grained angular sand at the base through coarse-grained silt in the middle section to fine clay, analogous to the host material — and color variations from olive-black at the base to olive-gray above. The textural features and the structure of the section indicate that the sand layer is, most likely, of turbidite nature.

Coarse-grained layers in the upper section rarely show a graded bedding. A typical example is a 1 cm

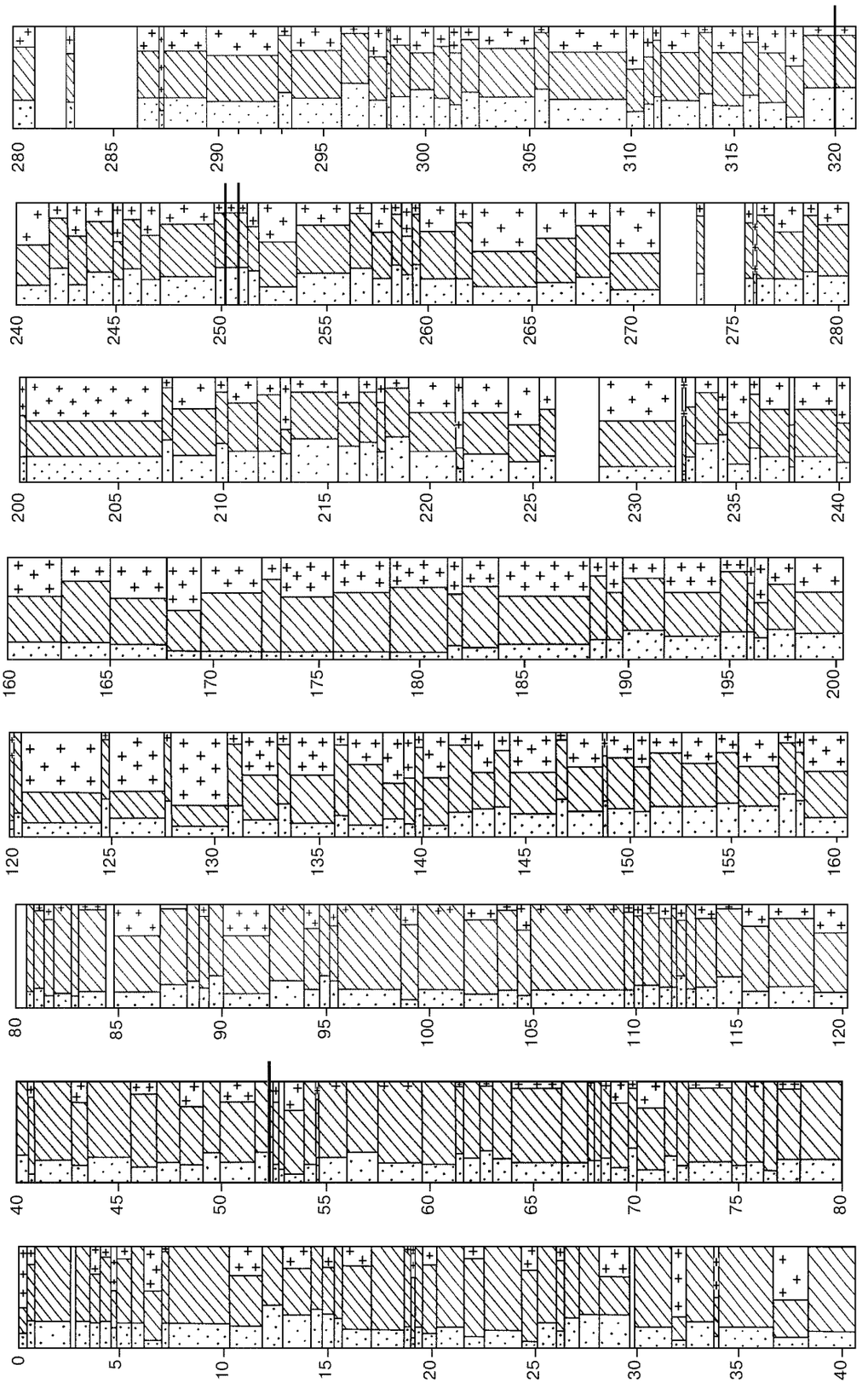
280 285 290 295 300 305 310 315 320
240 245 250 255 260 265 270 275 280
200 205 210 215 220 225 230 235 240
160 165 170 175 180 185 190 195 200
120 125 130 135 140 145 150 155 160
80 85 90 95 100 105 110 115 120
40 45 50 55 60 65 70 75 80
0 5 10 15 20 25 30 35 40

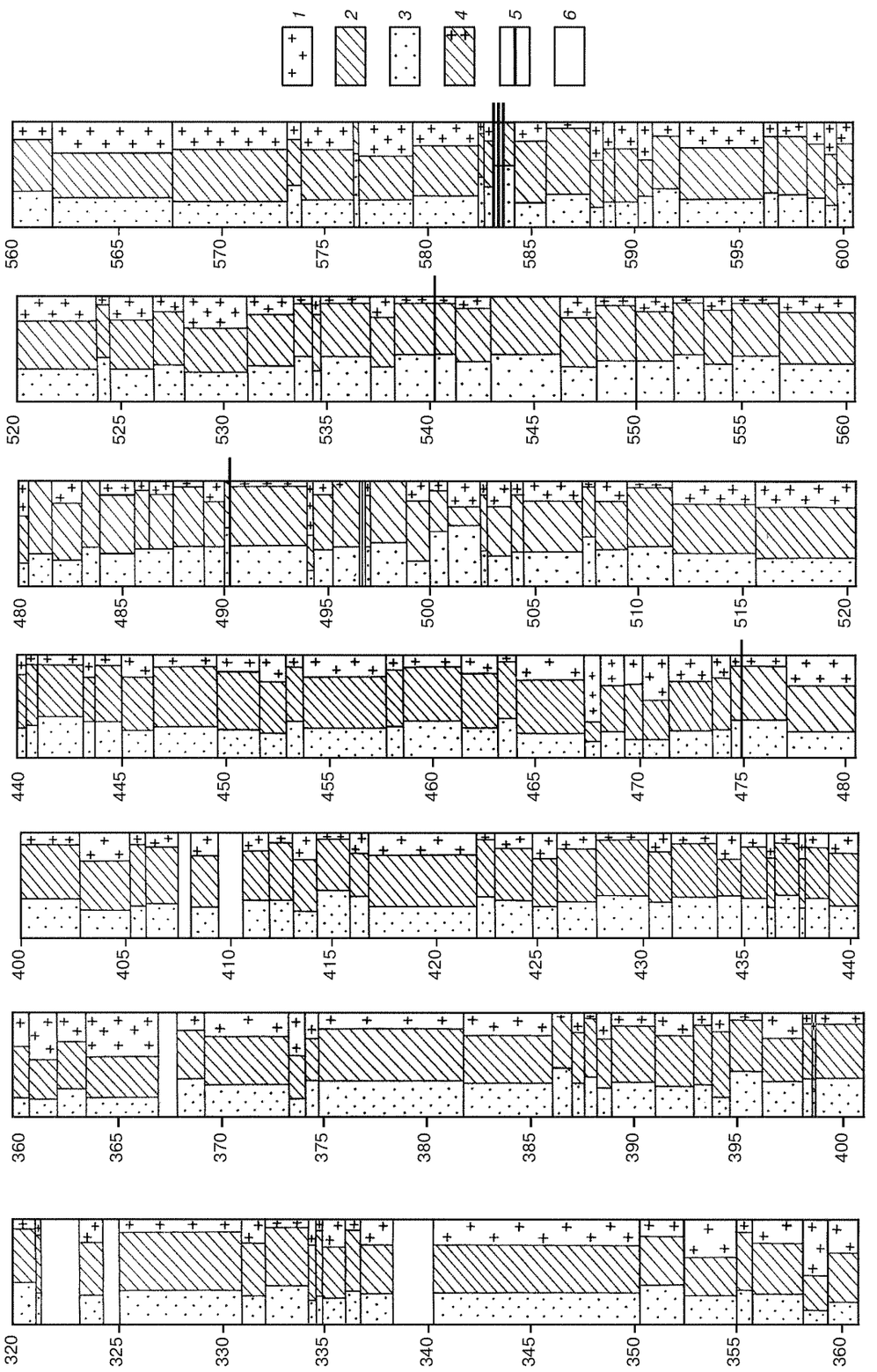

Fig. 3. Lithological profile of borehole BDP-98. *1* — diatoms; *2*, *3* — particles of clay (*2*) and silt-sand (*3*) size; (*1–3* show proportions of components in vol.%); *4* — diatom amount less than 3%; *5* — turbidite layers; *6* — core missing intervals. Digits on the right refer to subbottom depths, in m.

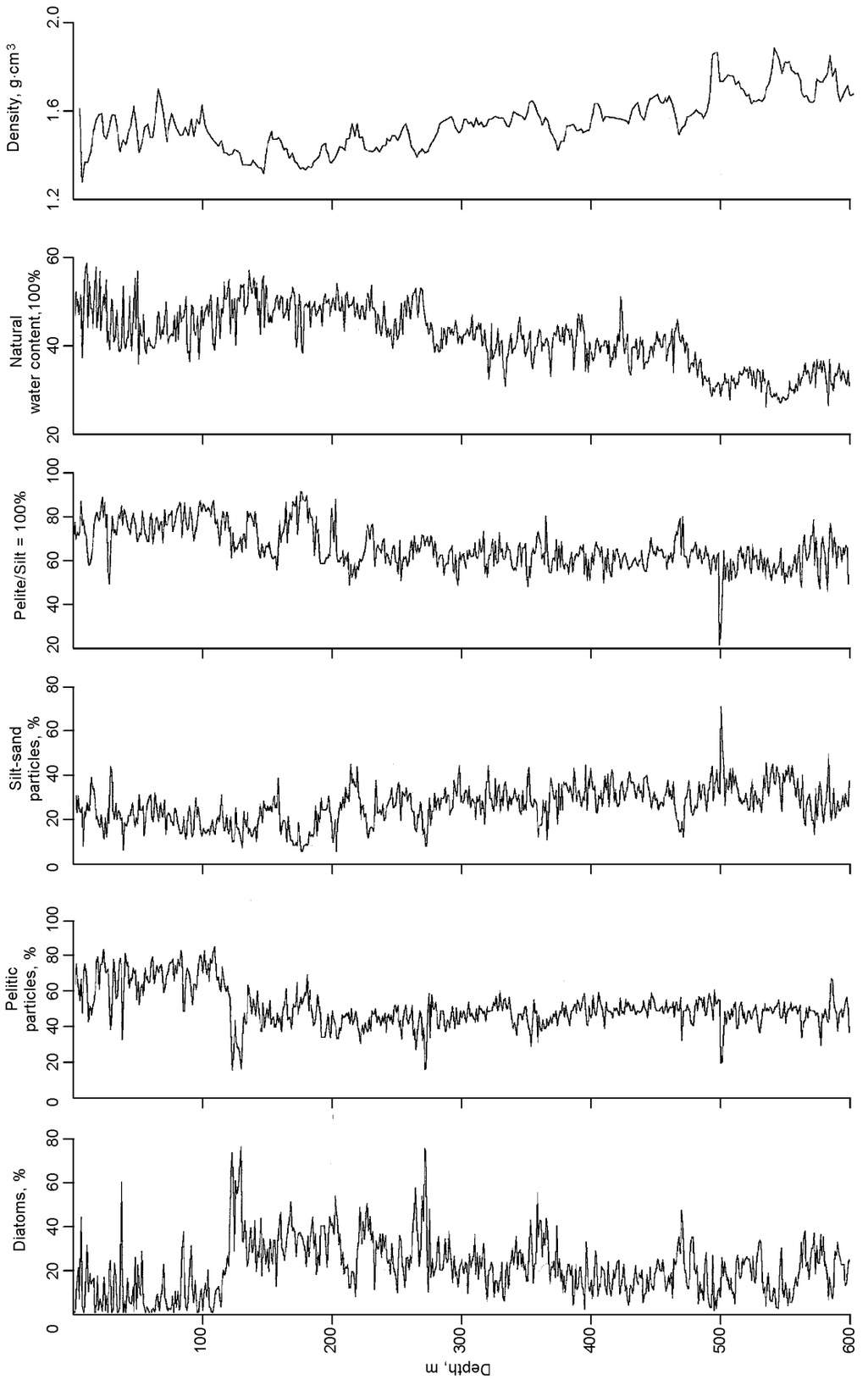

Fig. 4. Vertical variations of lithology and physical properties of sediments. *a* — diatoms; *b* — pelitic particles; *c* — silt-sand particles; *d* — proportion of pelitic and sand-silt particles, normalized to 100%; *e* — natural water content; *f* — density, in g/cm^3.

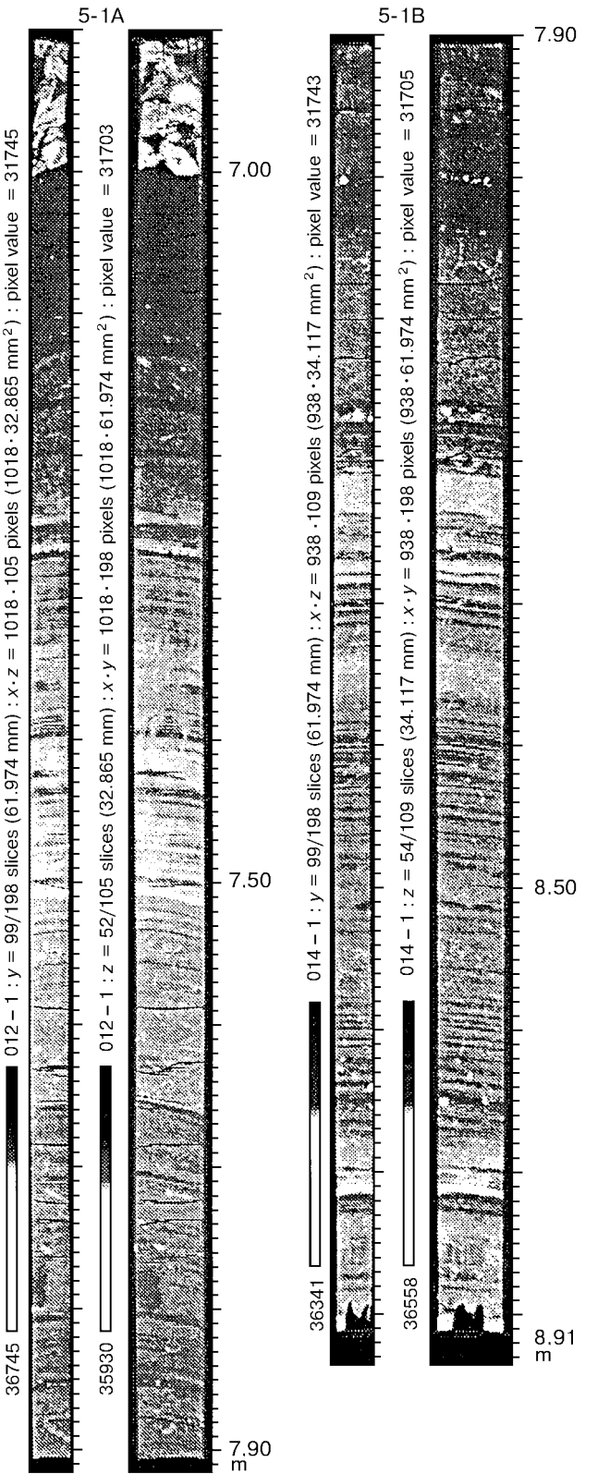

Fig. 5. Gamma tomography of core 5. BDP-98. Dark shade is diatom ooze; light shade is clay.

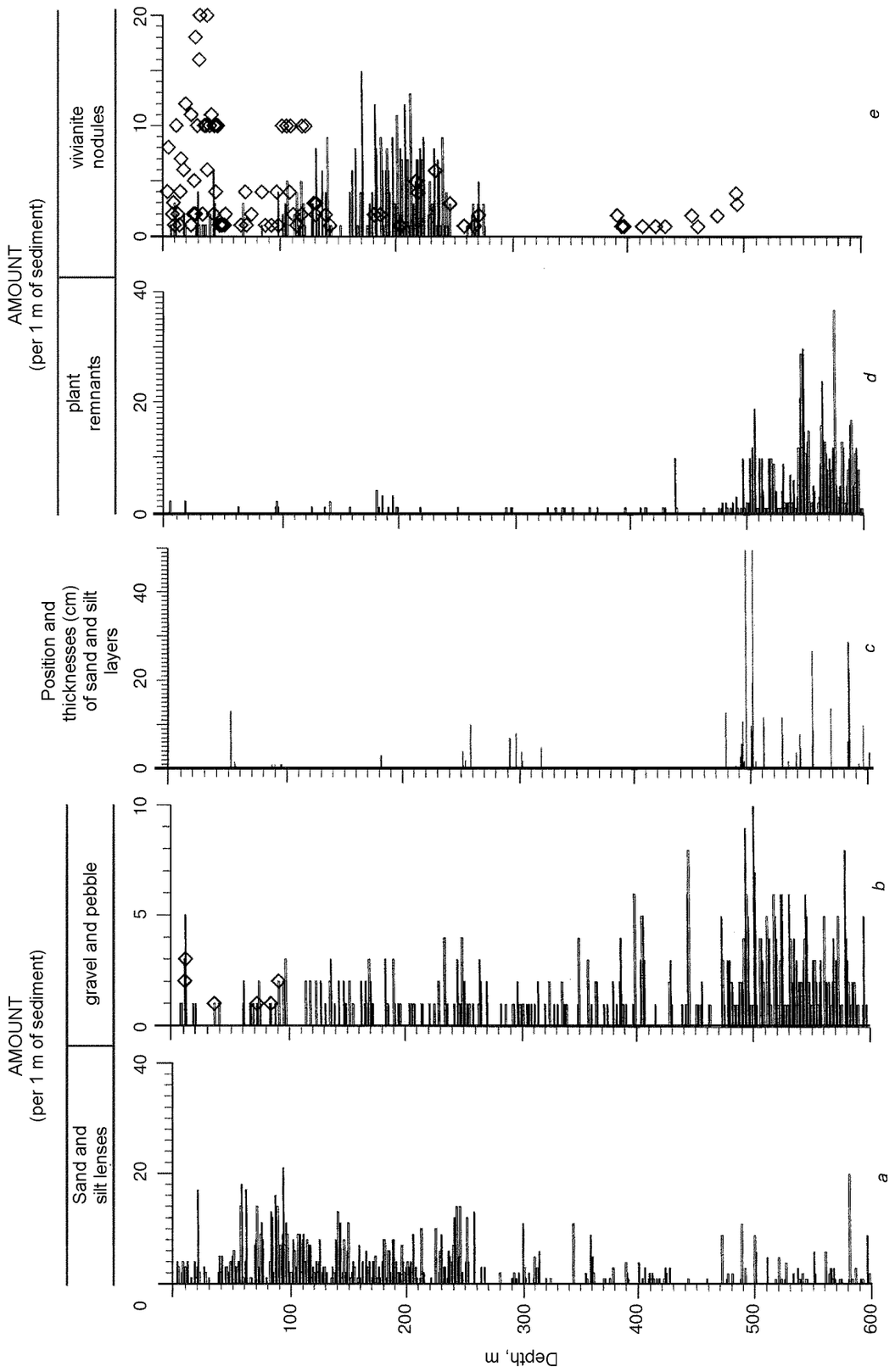

Fig. 6. Vertical distribution of: *a* — sand and silt lenses; *b* — gravel and pebbles (rhombs); *c* — position and thickness (cm) of sand and silt layers; *d* — plant remnants; *e* — vivianite nodules (rhombs).

Fig. 7. A green schist pebble with glacial striation, from a depth of 36.31 m.

thick layer at a depth of 55.45 m, composed of unsorted coarse sand. It has an uneven base, intervening as pockets or sags into the host clay. Although the proportion of clay material increases in the upper part of the layer, its upper boundary is distinct. Judging by its textural features, the layer cannot be turbiditic or produced by bottom water currents. Layers of this kind are rather large sand lenses produced by icebergs and ice rafting, which often occur in the upper part of the section, along with large outpinching lenses.

Turbidite layers more often occur below 250 m. Two 4 cm thick sand-rich silt layers were encountered at depths of 251.8 and 258.6 m, with distinct lower boundaries bearing traces of erosion. Sand exists as small horizontally positioned compact lenses related to bioturbation and is finer-grained upward, i.e., the lenses have a graded structure and are turbiditic. A clearly pronounced 8 cm thick turbidite layer at a depth of 297.32 m lies over an uneven eroded surface. It is composed of medium-grained sand below, fining upward and grading on into silt, and contains carbonified plant remnants. The upper part of the layer is silty-pelitic, with abundant small mica flakes. The upper boundary is obscure and transforms gradually into typical pelitic diatom ooze against which the turbidite stands out by much lower diatom contents (3% against 20–40%).

Turbidite layers encountered at depths of 475 and 492 m are composed of graded coarse material but include carbonate nodules, abundant sponge spicules, and minor mica flakes in the upper parts. The section below 500 m contains thick (1.5–1.8 m) sand-silt layers that have smooth boundaries with the over- and underlying sediments and show obscure layering produced by variations in sand content, which may attain 40%. The sediment matrix includes abundant plant remnants, which often make thin (1–5 mm) partings of horizontally lying carbonified leaves. The plant partings are associated with fine-grained sands and have clearly evident ripple marks on the upper boundaries (as, for instance, in the interval between 589.17 and 589.18 m).

The greatest portion of plant remnants in the section is concentrated in the lower 100 m (Fig. 6, *d*), where they are individual charred wood fragments (mostly above 550 m) or lenses and partings of carbonified leaves, mostly below 550 m (Fig. 8). One layer at a depth of 439.35 m contains both wood fragments and carbonified leaf remnants that make “a plant parting”. Plant remnants in the upper 370 m of the section exist as scarce small (0.1–1.0 cm) inclusions in the sediment matrix. The uppermost 100 m section contains wood fragments mostly within diatom ooze layers.

The lower 100 m section includes layers which can also be interpreted as turbidites. They differ in having sponge spicules and round carbonate nodules set in sandy matrix, most likely brought along with sands and plant remnants.

Vivianite nodules ($Fe_3(H_2O)_8[P_2O_4]_2$) are ubiquitous and exist most often in clay layers as tiny (0.*n* mm) spherical granules or segregations and aggregates, similar to vivianite nodules studied in the BDP-96 core [1]. The nodules are nonuniformly distributed throughout the core, being most abundant in the upper section, especially in the uppermost 50 m, and scarce to a depth of 490 m (Fig. 6, *e*).

Larger inclusions of vivianite occur as 2–5 mm (less often up to 1 cm) nests of irregular shape composed

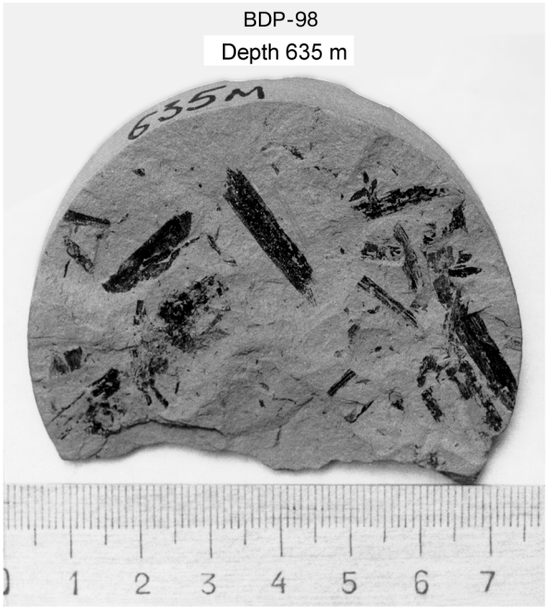

Fig. 8. Cross section of core BDP-98, from depth of 635 m. Dark patches are imprints of carbonified plants.

of grayish powdery material. In the air vivianite lenses change their color to bright-blue, which makes them easy to identify. These inclusions are encountered only above 270 m (Fig. 6, *e*), chiefly in diatom ooze, and are most abundant between 160 and 245 m.

The section also contains numerous bands, patches, mottles, and nests of hydrotroilite ($FeS \cdot nH_2O$) and separate pyrite crystals. The presence of hydrotroilite is well evident owing to dark, almost black, color of the core immediately after its recovery; hydrotroilite in nests exists as black powdery matter. In the dry core, hydrotroilite segregations acquire ochre-red colors.

It has been commonly believed that the Baikal sediments are free of carbonates. However, carbonate minerals were encountered below 100 m, being most abundant between 300 and 600 m. Carbonates exist as spherical micronodules (less than 1 mm in diameter) or as cement; in some veinlets their amount increases. Microscopy and X-ray spectroscopy showed that they are siderite ($Fe_2[CO_3]_2$) or rodochrosite ($(Mn, Fe)CO_3$).

Physical properties of sediments

Density of sediments was determined by weighing core samples (300–400 mg specimens) on torsion balance TB-500 in air and in kerosene. In total, measurements were carried out on 277 samples taken regularly throughout the section. The density values, with a temperature correction, range from 1.27 to 1.87 g/cm^3 (Fig. 4, *e*) and are highly variable because of variations in diatom abundance [1]. Diatom-rich layers are less dense than terrigenous clays, and the general tendency is an increase in density down the core. A strong decrease in density at depths between 120 and 140 m correlates with an abrupt increase in diatom content (Fig. 4, *a*). Below this interval, the average density increases monotonously with increasing consolidation of sediments. At the same time, the upper 100 m of sediments are obviously much denser than the middle section at the account of dense glacial clays. The lower 100 m of the section are the densest because of sediment compaction and a greater content of coarse material.

Natural water content in sediments was measured immediately after the core retrieval. Specimens of about 1 cm^3 were weighed, dried at 60 ˚C, and then weighed again. Sampling was performed throughout the core at every 10 cm. Water content in the 5530 samples we analyzed ranges from 17.12 to 73.93%, decreasing down the section (Fig. 4, *f*).

The water content profile includes several uniform intervals: Between 0 and 60 m, fluctuations are frequent and contrasting; from 60 to 270 m, they are less contrasting, but the average content remains nearly the same as above; from 270 to 470 m, the amplitude of fluctuations keeps decreasing and the average water content is

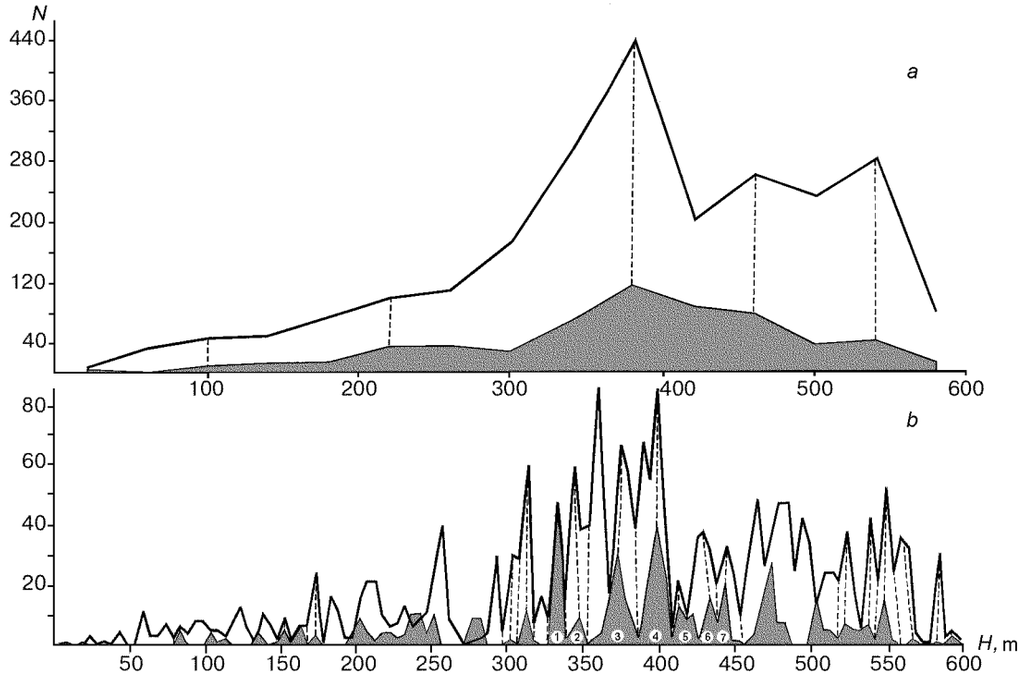

Fig. 9. Density of tension (white) and shear (dark) cracks (*N*) revealed in BDP-98 core. *a* — Averaged over 40 m; *b* — averaged over 5 m. Dashed line shows synchronous variations in densities of tension and shear cracks; numbers in circles refer to clustering zones of shear cracks.

lower than in the intervals above but remains invariable within the interval; between 470 and 600 m, the content of water is still lower and fluctuations are very weak.

Comparison of plots for fluctuations of density, water content, diatom abundances, and percentages of pelitic and sand-silt particles (Fig. 4, *a–e*) shows that each curve includes more or less similar intervals in which the plotted parameter is relatively constant. The reason is that these parameters are all related to sediment lithology and diatom abundance.

Evidence of faulting

Structural studies of the Baikal cores were undertaken for the first time during the 1998 experiment. Macroscopically examined, the BDP-98 core shows evidence of deformation not related to coring. The observed structural elements were typified on the basis of their morphology, and then their hierarchy and relationships were determined, as well as the character and the intensity of deformation of sediments. This preliminary analysis allowed a hypothesis of the origin of structures of different types.

The higher-order structures, broadly distributed below 50 m, are mostly of two types (Fig. 9). Those of the first type were identified as tension cracks (Fig. 10) produced by tectonic or, partly, diagenetic factors. Their size and formation mechanism indicate that no single deformation episode could lead to considerable dislocation of sediments, and perfect cementation is evidence for their present-day quiescence.

The structures of the second type are medium-size shear cracks [14] (Fig. 10), in most cases filled with hydrotroilite. They are less abundant than the tension cracks (Fig. 10) but are more important in the internal structure of the sediment. In spite of being latent because of a specific state of the host material, the shear cracks may cause an offset up to 20 mm (Fig. 10).

The cracks locally cluster into regularly patterned small zones (see Fig. 9, numbers refer to seven best documented zones), possibly formed during extension accommodated by normal faulting along conjugate shear cracks by the mechanism of double shearing [15]. The zones tend to the center of the more strongly deformed segment of the section (Fig. 9, interval 180–500 m), i.e., the borehole might have traversed a fault. Almost

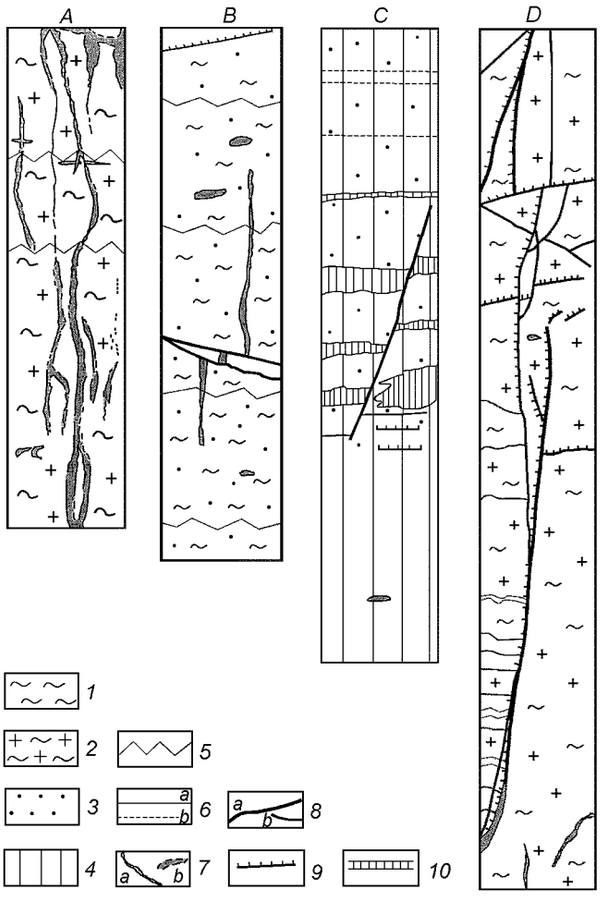

Fig. 10. Example documentation of cores with tension and shear cracks. *A* — Core 195, depth 356.08–356.50 m, *B* — core 187, depth 340.84–341.29 m, *C* — core 6, depth 9.25–9.78 m, *D* — core 202, depth 366.79–371.51 m. *1* — pelitic mud; *2* — diatom ooze; *3* — sand admixture in sediment; *4* — clay; *5* — core section breaks; *6* — clear (*a*) and poorly pronounced (*b*) layering; *7* — tension cracks (type 1) with clear (*a*) and poorly pronounced (*b*) boundaries; *8* — medium-size (*a*) and small (*b*) shear cracks (type 2); *9* — shear cracks filled with hydrotroilite; *10* — relatively large hydrotroilite partings.

undeformed horizontal lamination of the sediments, the absence of dragging features, etc., and a relatively small width of the fault indicate that it belongs to a larger scale structure, possibly produced by rifting-related motions of basement blocks. The same origin was inferred for similar on-land faults in the neighboring territories [16]. The effect of tectonic forces under these conditions is multiplied by the load of the overlying sediment and by fluid pressure strongly reducing the strength of the deformed material.

Taken together, the scarce and small faults do not cause much dislocation. At the same time, faulting must be of broad occurrence in the bottom sediments of Lake Baikal. The discovery of faults in the BDP-98 section opens new prospects for studies of active rifting, as in this case the process is not overprinted with effects of earlier structures. Further studies will allow an insight into features of faulting in the Baikal core, as well as into fundamental regularities of extensional tectonics. The results of structural studies should be taken into account in interpretation of depositional framework and in geological and paleoclimate reconstructions.

Geophysical logging

Geophysical logging (Table 1) included measurements of resistance (RL), self-potential (SPL), gamma

Table 1

Method	RL	SPL	GL	AL	IL	CRL	RTL	TM	IC	CV
Core depths	19–667	180–673	0–673	180–671	180–665	0–153	180–663	0–673	0–673*	0–673*

*** Measurements were also taken in submerged column above the bottom.**

radioactivity (GL), acoustic waves (AL), induction (IL), cement ring (CRL), resistivity (RTL), temperature (TM), inclination (IC), and cavernosity (CV).

Inclination measurements indicated a nearly vertical position of the borehole at angles within 1–2°. The submerged drilling column and the raiser of BDP-96 and BDP-98 departed from their original vertical position for 3–4°, or 15–17 m, at a water depth of 321–337 m, possibly because of horizontal shifting of ice blocks.

The diameter of BDP-98 slightly exceeds the nominal value throughout the section and narrows only when passing scarce thin permeable layers with infiltration crusts.

Acoustic logging was carried out by a log probe SPAK-6. The kinematic and dynamic parameters of compressional acoustic waves were measured in the interval from 180 to 671 m. Quantitative estimates were obtained only for depths between 483 and 671 m (denser rocks) because of technical limitations of the instruments (Fig. 11). However, as the measurements from the section above 483 m are of practical importance as well, they were co-processed with volumetric density data from the entire section (0 to 600 m, Fig. 4, *f*).

Velocities of acoustic waves in the section from 20 to 595 m were estimated from volumetric density of rocks measured on core samples (δ) using its statistical relationship with log traveltime of compressional waves (Δt) obtained for the interval of 483 to 595 m:

$$\Delta t = 770.563 - 113.638 \cdot \delta \ (r = -0.96).$$

The resultant velocities of compressional acoustic waves range as 1.6–1.8 km/s. Estimates of average velocities of elastic waves, with regard for water depth, allow more stable conversion of time- to depth-dependent seismic profiles (Fig. 11). The small value of sound velocity in the water (1430 m/s) was obtained by direct measurements by the log probe.

Radioactivity measurements were done by the gamma-log method, without using artificial sources. Gamma logging is an efficient tool to lithologically discriminate sedimentary rocks based on their natural radioactivity, which is relatively high in clay and the lowest in sand and sandstone. Silt, argillaceous and silty sand have intermediate values of radioactivity, as well as diatom-rich sediments [1].

As a result of gamma logging, the section was divided into segments with low, intermediate, and high radioactivities (Fig. 12). Vertical radioactivity variations reflect the lithological inhomogeneity of the section. Segments of relatively uniform behavior and average values of radioactivity generally coincide with the intervals on the diatom abundance plot: 0–110; 110–150; 150–270; 270–480; 480–610 m. The radioactivity intervals to a depth of 480 m may be controlled by variations in diatom content. At the same time, a greater radioactivity in the lower section might be somehow related to a greater proportion of sand, but this requires further studies.

The self-potential method (SPL) provides information about lithology of rocks and their permeability and store capacity. Synthetic processing of SPL and gamma-logging data confirmed the existence of interfaces at 270 and 476–480 m.

Temperature measurements in the borehole were taken continuously by well resistivity thermometers at a resolution of 600 m/h (Table 2).

Since the temperature logging was performed immediately after the cessation of drilling (preliminary recovery of the borehole never exceeded 36 hours), thermograms show a strongly unsteady temperature field

Table 2

BDP-98	Subbottom measurement interval, m	Temperature (from – to), °C	Average geothermal gradient, mK/m
Hole I	0–149	4.3–9.45	25.9
Hole II	0–673	4.3–31.75	40.8

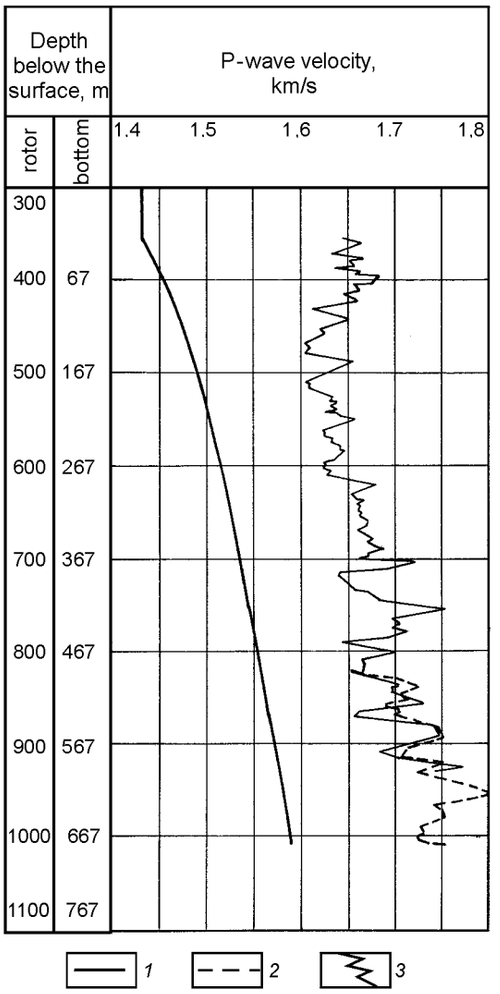

Fig. 11. P-wave velocity profile. *1* — average P-wave velocity in wet sediment; *2* — P-wave velocity, from acoustic log; *3* — P-wave velocity, from sediment density estimated on core samples.

disturbed chiefly by well flushing. However, a steady-state geothermal gradient can be obtained from a nonsteady thermogram using modern interpretation methods [17]. A temperature curve from the second hole recorded during the sinking of the drill was processed by the program ONELOG kindly offered by I. M. Kutasov. A steady-state geothermal gradient was obtained for core depths of 30 to 500 m; temperatures measured at 0–30 m, subject to bottom effects, and below 500 m, distorted by changes in drilling velocity, were excluded from processing. The calculated steady-state geothermal gradient in the upper 500 m of sediments averages about 60± 10 mK/m. The corresponding steady-state bore-face temperature must be 43–44 °C, which is 12–13 °C higher than its measured values.

Thermal conductivity of sediments

Thermal conductivity of the retrieved BDP-98 core was measured by a needle-probe (252 measurements) and by a thermal conductivity comparator (1391 measurements). The needle-probe method has been in use for more than 40 years in thermal conductivity measurements of oceanic bottom sediments [18]. The thermal conductivity in the BDP-98 section above 350–400 m varies very little and averages about 0.95± 0.10 W/(m· K), which is in good agreement with the previous measurements of the 100 m thick BDP-96-2 core [1]. At greater

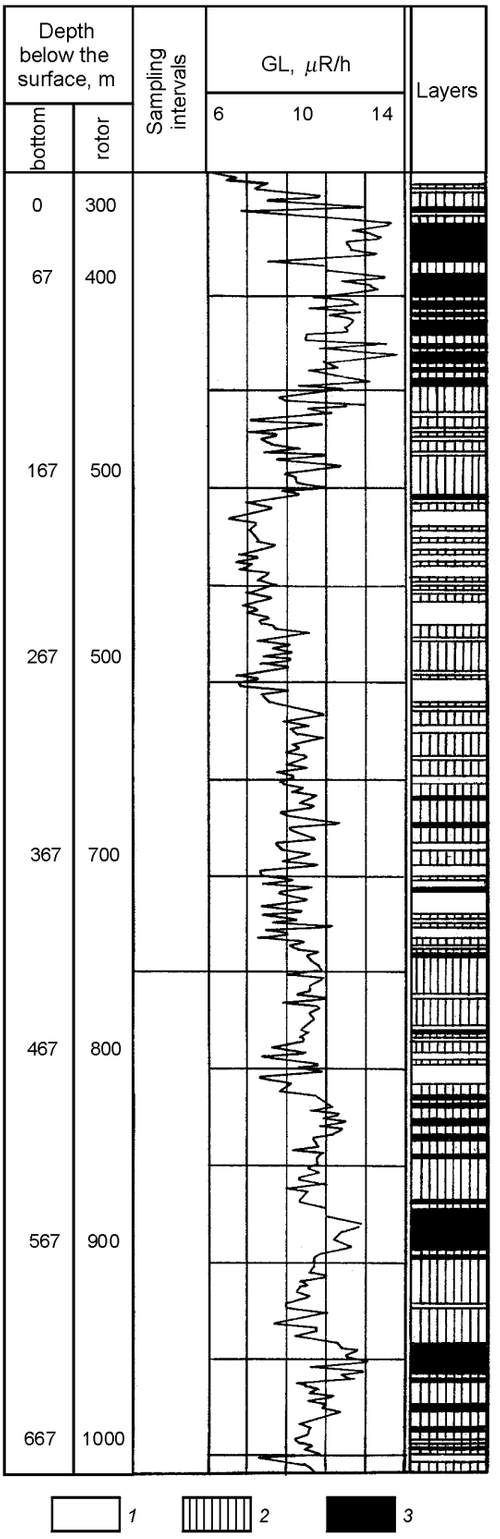

Fig. 12. Gamma log. BDP-98. Division of the section on the basis of natural radioactivity: *1* — low; *2* — intermediate; *3* — high.

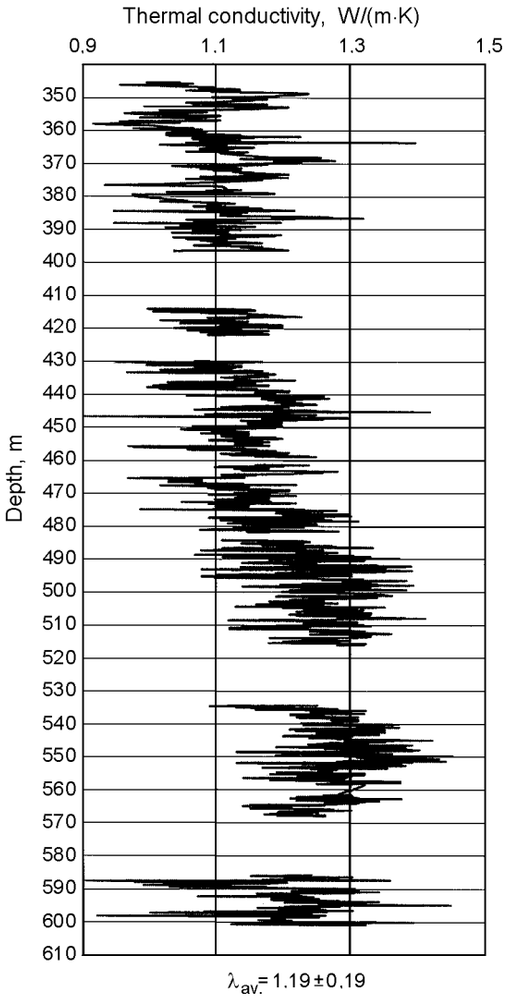

Fig. 13. Thermal conductivity of sediments. Measurements by thermal conductivity comparator at depths from 345.2 to 600.9 m.

core depths (400 to 600 m), thermal conductivity increases to 1.19± 0.14 W/(m· K). The measured thermal conductivities are in line with data on water content and density obtained for the same samples.

The measurements by a thermal comparator, calibrated against standard thermal conductivity samples in the range of 0.2 to 14.7 W/(m· K), were performed in the depth interval from 345.215 to 600.925 m. The advantage of this method is that the sediment is preserved intact, as measurements are taken on the surface of core samples split in halves on the long axis. Statistical processing (Fig. 13) included 1382 measurements, 9 samples failed the 2σ error criterion and were deleted. The average thermal conductivity coefficient ($\lambda\pm 2\sigma$) over 1382 measured values is 1.19± 0.19 W/(m· K), and the range is from 0.88 to 1.44 W/(m· K). The latter extreme values are single and not typical. The typical values are about 1.1 W/(m· K) at depths from 345 to 440 m, then increase (1.25–1.30 W/(m· K)) to a depth of 555 m, and then decrease slightly to 1.20–1.25 W/(m· K) at 600 m.

The average thermal conductivity of sediments measured in BDP-96-1 was 1.24± 0.19 W/(m· K) (from 512 measurements). Thus, the results of the two experiments nearly coincide (to 0.1 W/(m· K)), though the number of measurements in BDP-98 is nearly three times as great.

The detailed thermal conductivity studies provided a basis for heat flow estimation. With the average thermal conductivity of 1.10± 0.12 W/(m· K) in the interval of 0 to 500 m and the average geothermal gradient

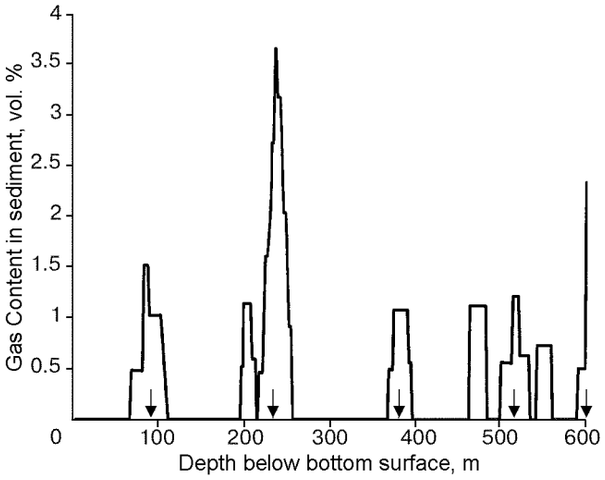

Fig. 14. Gas content. BDP-98. Arrows show sites of sampling for chromatographic analysis.

of 60± 10 mK/m (see above), the average heat flow for BDP-98 is 66 mW/m^2. Shallow heat flow measurements on the Akademichesky Ridge yielded generally high values, from 60 to 100 mW/m^2 [1]. The mean heat flow estimated for the BDP-96 borehole (for depths from 0 to 100 m) was 65 mW/m^2 [1]. Therefore, the average heat flow value obtained for the BDP-98 borehole agrees with the previous data for this part of the Baikal bottom.

Gas composition

Gas samples were taken throughout the BDP-98 section. The contents of main gas components were determined immediately aboard the drilling complex, but the greatest portion of analytical work was carried out in laboratory. Gas samples were transported in special containers which proved efficient in the experiments of 1996–97.

In the upper part of the section (to 200 m), gas release from the core was very weak (no more than 5–10 ml from a core 200 cm in length and 54 mm in diameter). Therefore, the existing system of sampling failed to provide high-quality samples. The quality was determined by the percentage of oxygen, and the samples that contained over 5% of oxygen were deleted. (Note that, during the previous experiment, 2 l of gas released from a core of similar size from a depth of 120 m in BDP-96 located about the same site as BDP-98.) Porosity and gas content of the core were then estimated on the basis of density and water content measurements (Fig. 14).

The samples were analyzed for He, H_2, O_2, N_2, CH_4, C_2H_6, and CO_2. The content of helium in the gas mixture freely released from the core varies from 6 to 36 ppm (the content of He in the air is 5.2 ppm) and increases downcore; the content of hydrogen is 31 to 652 ppm (0.55 in the air) and is strongly variable throughout the section. The concentration of carbon dioxide averages about 5.3 vol.% and virtually does not change with depth (its concentration in the air is 0.035%). The content of nitrogen, converted to air-free content, is 1.5 vol.% in all samples. The content of methane, which is the main component of the gas mixture, attains 86.56–91.68 vol.% (average 88.37 vol.%). Ethane makes 899–1058 ppm.

The CH_4/C_2H_6 ratio is below 1000 and ranges between 769 and 962 in all samples except for one from the depth of 250 m, in which this ratio is 1020.

Carbon isotope ratios in CO_2 and methane vary from –3.7 to –8‰ and from –67 to –70‰, respectively. There is a linear correlation between $\delta^{13}C(CH_4)$ and $\delta^{13}C(CO_2)$, which indicates a single source of the gases. In marine sediments, $\delta^{13}C(CH_4)$ is 50 to 80‰, and if it is below –58‰, methane is interpreted [3] to be of biogenic origin. The measured values of $\delta^{13}C(CH_4)$ in the gas samples taken in the South basin (BDP-97; $\delta^{13}C(CH_4)$ = –70.4…–74.6‰) and in the central part of Baikal (Akademichesky Ridge) are all within the range of –67…–74.6‰ , thus indicating the biogenic origin of CH_4.

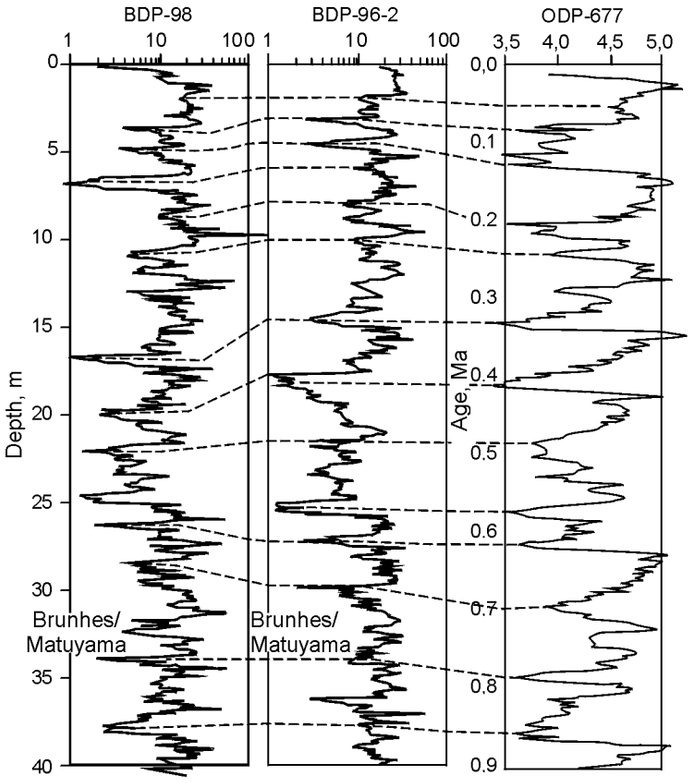

Fig. 15. Correlation of whole-core magnetic susceptibility profiles ($K = 10^3$ SI units) for cores of BDP-96-2 and BDP-98 and ODP-677 oxygen isotope record (on the right), for upper 40 m of bottom sediments [22]. Correlation lines (dashed) tie characteristic peaks. Plots illustrate possibility to use Baikal magnetic susceptibility profiles as a climate proxy, as was proved earlier [19–21]. Note that upper 0.5 m section is not included, and the first warming stage is not so clearly pronounced.

The $^3He/^4He$ ratio ranges from 0.226 to $0.473R_{atm}$. These low "crustal" values agree well with heat flow values of 60 to 70 mW/m^2 [1] measured in the region of drilling, which is evidence of the absence of heat and mass transfer from the bedrock on the Akademichesky Ridge.

Studies of paleomagnetism and magnetic properties of rocks

It was shown that magnetic susceptibility, which reflects concentration of magnetic minerals in rocks, can be used as a proxy of paleoclimate in the Baikal sediment record [4, 19–22]. Whole-core low-field magnetic susceptibility (K) of sediments was measured at 3 cm intervals with a Bartington Instruments pass-through loop sensor, and the results were used for preliminary magnetostratigraphy. The BDP-98 cores retrieved by piston and rotary coring match in quality the best ODP cores. The full-scale processing is still under way, but preliminary results show a good correlation with the magnetic susceptibility profiles for the earlier BDP-96 cores and with the ODP-677 oceanic oxygen isotope record (Fig. 15). According to the BDP-98 magnetic susceptibility profile, which provides a faithful record of climate changes, the Brunhes/Matuyama boundary (780 ka) must be at about 34–35 m of the core depth.

For paleomagnetic study, the core was sampled at 5 to 15 cm intervals, and the oriented sediment samples were placed into 5 cm^3 cubic plastic boxes. Stepwise alternating field (AF) demagnetization of samples has been completed by now for the upper 300 m of sediments. Figure 16 shows an example of AF cleaning for samples from depths of 4.95 m (Brunhes Chron, direct polarity) and 37.01 m (Matuyama Chron, reverse polarity). The optimum blanket demagnetization field, determined on the basis of cleaning of pilot samples,

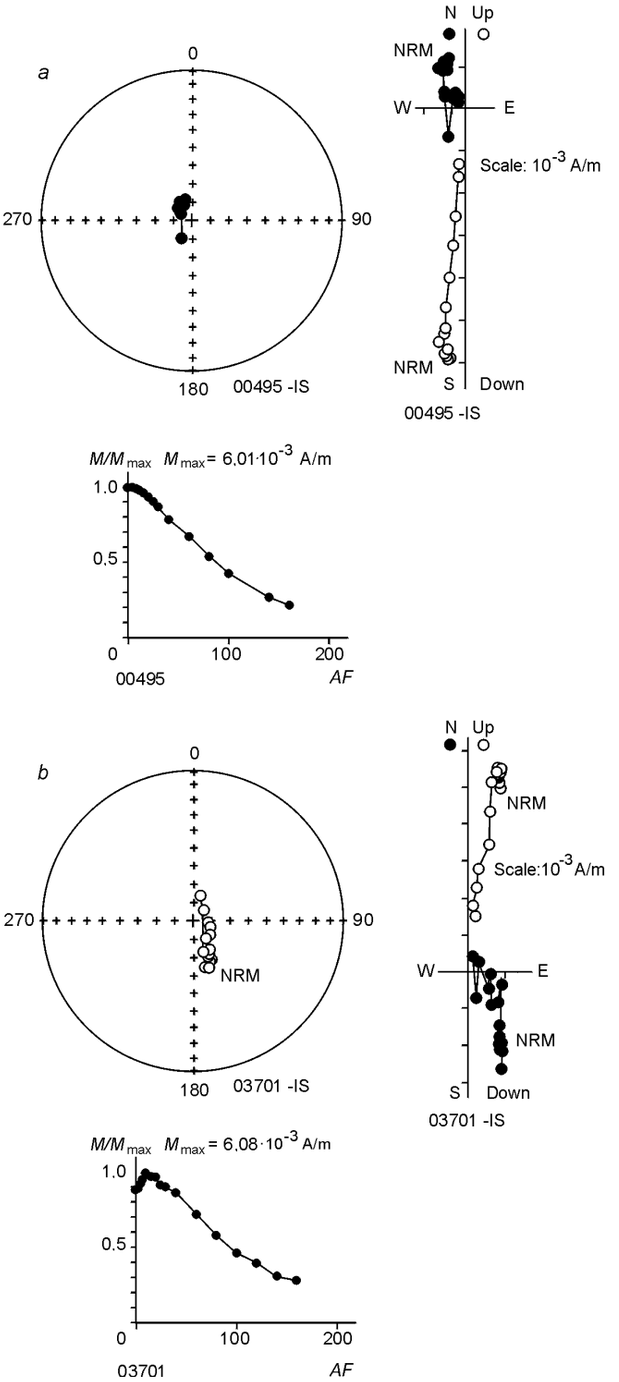

Fig. 16. Typical AF demagnetization plots (Russian data). Pilot samples from BDP-98 core: *a* — 4.45 m, Brunhes Chron; *b* — 37.01 m, Matuyama Chron. Stereoplots (on the left) and Zijderveld plots (on the right) show vector directions in space. Open (bold) circles on stereoplots mark positive (negative) NRM direction; bold circles on Zijderveld plots are orthogonal projections of remanence during cleaning, in Cartesian coordinates (e.g., N is direction to the north, E is direction to the east); open circles correspond to vertical projection (Up means negative direction upward, E is direction to the east). NRM marks the onset of demagnetization. M/M_{max} (*AF*) plot is normalized NRM vector as a function of demagnetizing field, mT.

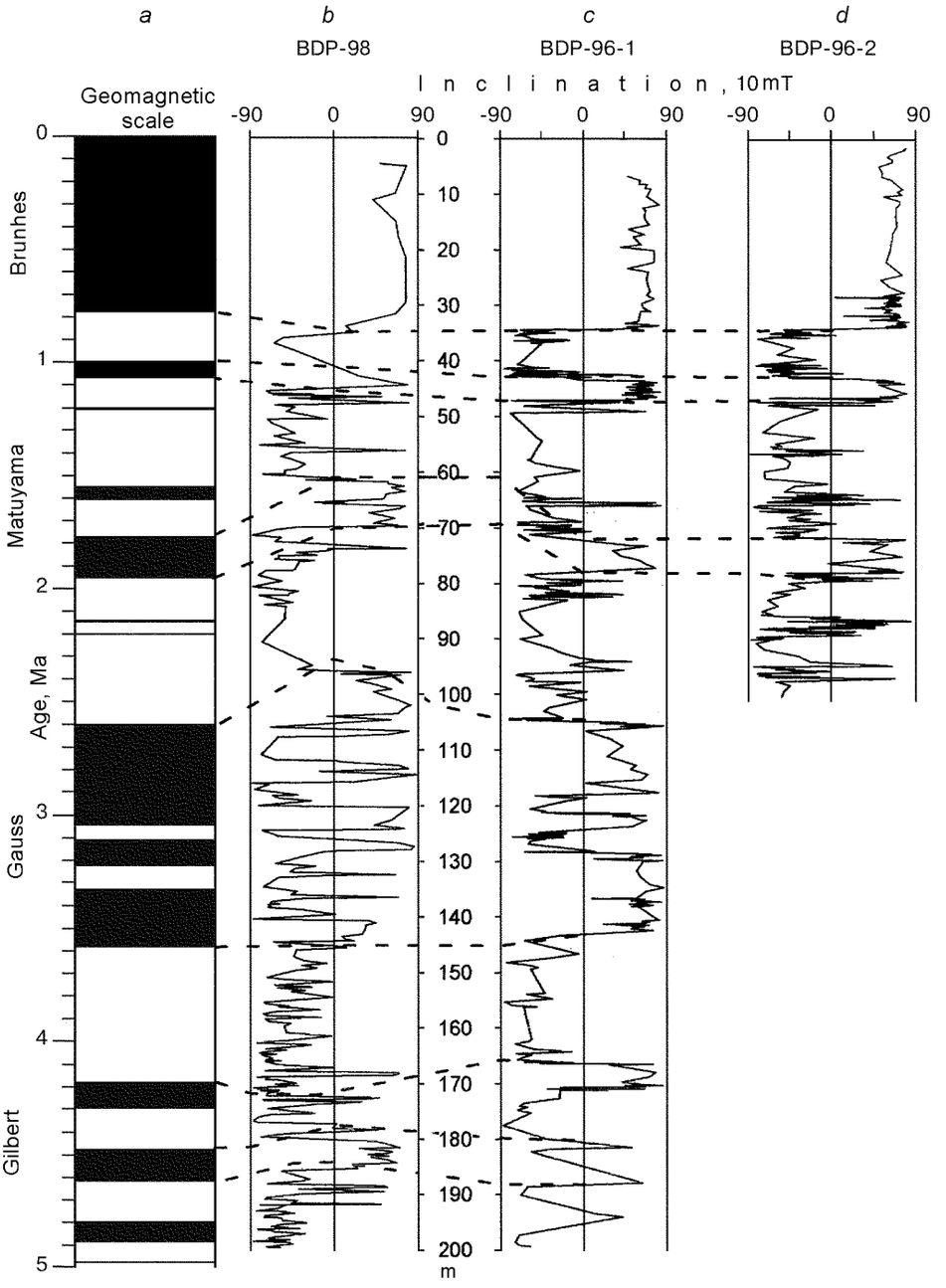

Fig. 17. Preliminary magnetostratigraphy for the last 5 Ma (Russian data), from studies of cores from BDP sites on the Akademichesky Ridge. *a* — Geomagnetic polarity time scale, after [22, 23]; inclination plots for BDP-98 (*b*), BDP-96-1 (*c*), and BDP-96-2 (*d*) cores after AF demagnetization at 10 mT. Correlation tie lines (dashed) illustrate good core-to-core agreement. Note significant depth misfit of some polarity chrons in spite of general correlativity of geomagnetic episodes.

was 5, 10, 20, and 40 mT. At low demagnetizing fields (5–20 mT), data contain a viscous remanence component, which is produced by modern remagnetization overprints (Fig. 16) and is removed at fields between 10–20 mT.

Figure 17 shows a preliminary NRM record of samples demagnetized at the optimum blanket field of 10 mT, for part of the collection. The signal looks noisy, because not all failed samples (subject to sampling and measurement errors) have been deleted and the lithologic correlation is still incomplete. The geomagnetic time scales based on demagnetized samples of the BDP-96 and BDP-98 cores show a good general correlation with each other and with the world geomagnetic time scale. The Brunhes/Matuyama boundary is at nearly the same depths (34–36 m) in records from different boreholes, though there is some discrepancy (up to 10 m) between the BDP-96 and BDP-98 records for a number of events.

The paleomagnetic study of the BDP-98 core provides a reliable age of 6.56 Ma for sediments at a depth of 277 m. Below this depth, interpretation of the available data is problematic and requires further investigation.

DISCUSSION

Dating of sediments at the end of the section

Thus, according to the rock magnetic record, the age of sediments at a depth of 277 m is 6.56 Ma. The average sedimentation rate during that time span was 4.22 cm/1000 years, which is about that estimated for the BDP-96 core, Akademichesky Ridge (4 cm/kyr) [1]. The slightly greater value for the BDP-98 core correlates with greater thicknesses of sediment layers, which is seen in the seismic profile (Fig. 2) showing the position of the two boreholes. With a whole-section extrapolation, this average sedimentation rate yields an age of 14.5 Ma for a depth of 600 m. However, lithological evidence indicates a downward coarsening of sediments and the presence of sand layers and turbidites in the lower part of the section, which corresponds to more rapid deposition and, hence, a younger age at the borehole face.

Below the paleomagnetically constrained depth (277 m), the age of sediments was estimated using correlation with periodic changes in the Earth's orbital parameters. As known [22], and as was shown for the BDP-96 core [4], the paleoclimate record exhibits orbital cycles of 100, 41, and 23 ka. They are best evident in the biogenic silica record obtained for BDP-98 at a sampling rate of 10 cm. The $bSiO_2$ spectra correlate well with the paleomagnetic record within the time span from 0 to 6.56 Ma and the depth interval of 0 to 277 m, and below they are somewhat stretched. The record could be brought in agreement with the orbital cycles by compression along the time axis. Because of nonuniform sedimentation rate in the lower section, this procedure was performed separately for several depth intervals.

As a result, the sedimentation rate for the interval from 280 to 400 m was estimated at 5.5 cm/1000 years. Therefore, the sediments at a depth of 400 m must be 8.8 Ma old. In the interval of 400–480 m, the rate increases to 13.7 cm/1000 years, and the age of the sediments at 480 m is correspondingly 9.4 Ma. We failed to distinguish orbital frequencies below this interval, possibly, because of strong fluctuations of sedimentation rate. If we estimate the age of the lowermost 120 m by extrapolating the sedimentation rate of the previous interval, the age of the sediments at 600 m will be 10.3 Ma, which is obviously somewhat overestimated.

Interpretation of seismic data

The experiment of 1998 included seismic stratigraphy, i.e., tracing stratigraphic boundaries from seismic velocities in sediments [8]. Figure 18 shows the position of acoustic boundaries and the true depths calculated from average seismic velocities based on acoustic log data (Fig. 11). Boundary B10 in BDP-98 is at a core depth of 100 m, and B6 is at 560 m, if we accept the interpretation suggested in [24]. According to [7] and [8], these are principal acoustic boundaries related chiefly to erosional unconformities. However, the existence of erosional boundaries is not supported by lithological evidence. Significant changes in sediment lithology occur at 110–120 m and are associated with an abrupt decrease in diatom abundance in the upper part of the section and with the appearance of dense glacial clays. The acoustic boundary must be produced by sediment compaction rather than by erosion, which is well illustrated by an increase in density from 100–130 m (see the density profile in Fig. 4, *e*).

Note that the position of the boundary B6 in the drilling site has been interpreted ambiguously. Seismic profiling shows a thickly layered unit at depths of 470 to 560 m, and below 560 m, the seismic section is still more thickly and distinctly layered. Lithological evidence indicates considerable changes in sediment properties below 480 m, marked by an increase in density (Fig. 4, *e*), a decrease in water content (Fig. 4, *f*), and the appearance of turbidite and sand layers (Fig. 5, *c*) and abundant plant remnants and gravel (Fig. 6). This means that the boundary of deltaic deposits is at a depth of about 480 m. The position of the acoustic boundary B6 on the seismic profile corresponds to 560 m and is related to a change in density. Moreover, the seismic

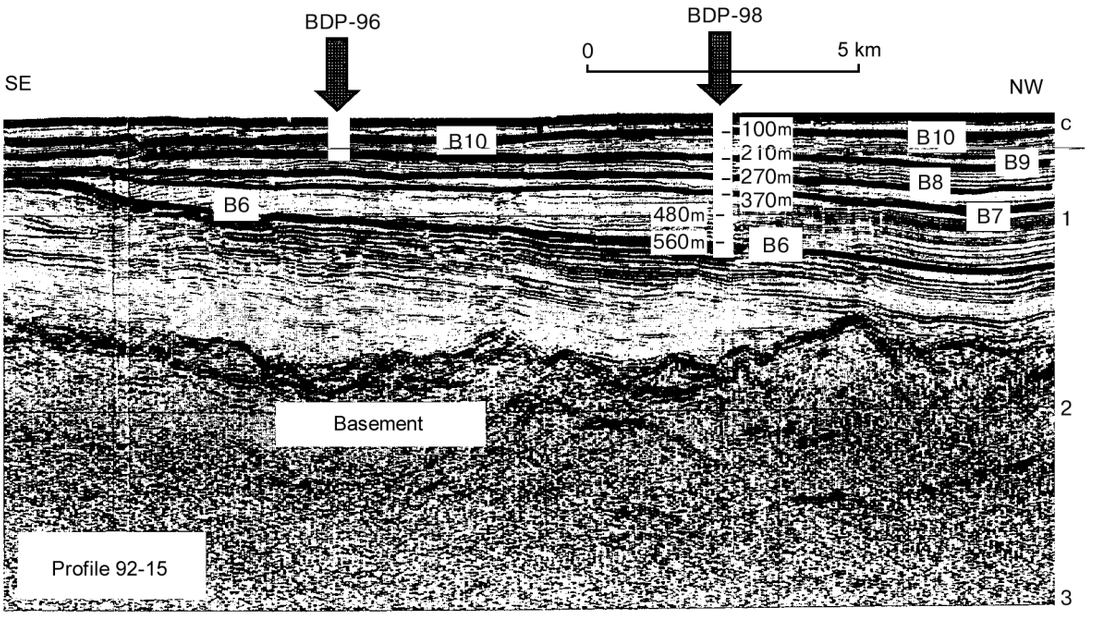

Fig. 18. Interpretation of seismic profile 92-15 (see Fig. 2). Shown are acoustic boundaries in the lower (Barguzin) sequence (B6–B10). White columns show drilling depths of BDP-96 and BDP-98. Digits in the BDP-98 column refer to subbottom depths of acoustic boundaries, calculated from acoustic log data. Note well-evident wedge-like deltaic deposits of the Paleo-Barguzin in the left top corner.

profile shows other acoustic boundaries at 370 (B7), 270 (B8), and 210 (B9) m, which coincide with lithological and physical boundaries. The horizon of 270 m is marked by a decrease in average diatom abundance (Fig. 4, *a*) and an increase in percentage of coarse particles (Fig. 4, *d*), which causes sediment compaction (Fig. 4, *e*) and, apparently, determines the changes in the seismic pattern. The 270 m boundary is also associated with a notable decrease in water content (Fig. 4, *f*) related to the decrease in average content of diatom frustules (Fig. 4, *a*). The boundary at 370 m is marked by a greater abundance of diatoms (Fig. 4, *a*) and the related decrease in sediment density (Fig. 4, *e*). Note that the interval of 270–370 m showing weak fluctuations of sediment density is viewed in the seismic profile as a continuous nonlayered acoustically transparent unit.

Thus, the lithology and physical properties of the sedimentary section of the Akademichesky Ridge agree well with seismic-profiling data. The best accord is between seismic boundaries and density variations, which is quite reasonable, as elastic-wave velocities are proportional to density.

Boundary B10 is distinctly evident in all basins of Baikal [6–8] and has been interpreted to mark the onset of the Neobaikalian stage in the rift evolution [8], assigned to the late Lower-early Upper Pliocene (3.5 Ma) [10, 25]. This stage is associated with intensification of tectonic activity, namely, subsidence of basin floors and uplift of mountainous rift shoulders [25]. The depth of B10 shows strong lateral variations over the Baikal basin: It is 1500–1700 m in the North basin [8], 100–120 m on the Akademichesky Ridge at the 1996 and 1998 drilling sites, and 300 m in the Central basin. According to geophysical evidence [7, 8], the upper unit above B10 rests unconformably over the underlying sediments truncating their cross-bedded layers. The results of drilling on the Akademichesky Ridge do not indicate any notable evidence of erosional unconformity [1]. At the same time, as written above, notable environmental changes in the early Upper Pliocene are recorded as a sharp decrease in proportion of biogenic material and the appearance of fine-grained highly dense clays in the upper section. The clays appear to be of glacial origin and are virtually barren of diatom frustules, unlike the sediments below (Figs. 3, 4, *a*). The age of the boundary B10 is 2.5–2.8 Ma, as estimated from timing the BDP-96 [1] and BDP-98 (Fig. 17) sections, which apparently corresponds to the onset of the Neobaikalian stage [10, 25] associated with more active subsidence of the Baikal basin. This subsidence is especially well evident in seismic profiles of the North basin [7, 8], and the sediments then deposited make a typical basin fill complex of the late rifting stage [7].

At the same time, the boundary B10 on the Akademichesky Ridge, where it is at a depth of 100–120 m, is related to climate-controlled changes in sedimentation caused by cooling, as reflected in an abrupt decrease in bioproductivity (lower diatom content) and the appearance of glacial clays [26]. It can be hypothesized that the climate change and the tectonic events at the boundary of 2.5–2.8 Ma may coincide. By that time, the mountain ridges around the Baikal basin may have risen high enough to be covered with glaciers. Thus, the Neobaikalian stage of the region evolution was marked by the uplift of mountains.

The depth variations of B10 and, hence, the thickness variations of the upper seismic unit are caused by variability of basement subsidence rate and of sediment supply. The high and medium (to 64 cm/1000 years) sedimentation rates in the North basin are due to both rapid subsidence and broader occurrence of glaciers in the bordering mountains during the Sartan glacial, as compared to the surroundings of the South and Central basins [25]. The role of glacial material in the North basin fill is, in our view, very important. As known, Selenga, the largest river supplying 80% of sediment into Baikal, is now responsible for about 60% of solid load input into the Central basin [27, 28], and the Upper Angara, the largest inflow into the North basin, brings no more than 10% of the solid load. At the same time, the sediment thickness of the upper seismic unit in the North basin is over 5 times as great as that in the Central basin. Therefore, the main influx of sediment material into the North basin must have been due to glaciers for the last 2.5–2.8 Ma.

Interpretation of depositional environments at the drilling site

Variations in lithology and physical properties of sediments are expressed in the section in a number of uniform layers whose boundaries are consistent with seismic stratigraphy. At the same time, the lithological profile does not show evidence for sedimentation gaps. The entire sequence we studied deposited in a water basin, which is confirmed by the absence of gaps, as well as by the gray ("reduced") color of sediments and by the absence of oxidized subaerial facies. The boundaries that divide the section into several layers are related primarily to environment changes controlled by climate and sediment supply.

The lower section (600–480 m) at the drilling site differs strongly from the upper one, chiefly, in greater content of silt, sand, and gravel material. This depth interval is also characterized by the presence of abundant plant remnants, sand-silt layers, and turbidites, a much lower water content, and a greater density of sediments (Figs. 4 and 6). These specific features may be due to the position of the drilling sites near the shore, not far from a large source area, possibly the delta of a large river well pronounced in seismic profiles (Figs. 2 and 18) [8], maybe the Paleo-Barguzin [5]. This layer, possibly, deposited at some distance (12 km) away from the river mouth and may be syngenetic to the deltaic facies. The drilling site is located on the submerged slope of the delta, on the slope rather than on the bottom of a 200–300 m deep sedimentation basin, which is indicated by scarcity of turbidites or thick beds of coarse sediment. Our data support the interpretation by Moore et al. [8], who suggested the existence of a deep basin during the formation of B6.

The abundance of gravel (Fig. 6, *b*) in relatively fine-grained host sediment suggests a special mechanism of sediment transport. Ice rafting fails, as the climate conditions were subtropical. Sediments (gravel-bearing soil) may have been transported on plant roots brought by the river. The presence of sand- and silt-rich layers smoothly grading into a finer-grained matrix may attest to fluctuations of lake level.

The lowermost section (560–600 m), corresponding to B6, is the richest in plant remnants (Fig. 6, *d*), especially leaf fragments, possibly because the source area approached the site of drilling during the basin shoaling.

The sediments between 480 and 270 m have constant water contents and percentages of coarse and pelitic particles (Fig. 4). This section may have deposited in stable conditions. At the same time, it contains a diatom-rich and a diatom-poor subunits (480–370 m and 370–270 m, respectively), also distinguishable on the density curve (Fig. 4, *e*), with a minimum at 370 m. The section may have deposited far from the direct influence of river discharge, in a progressively broadening and deepening water basin, as its shores appear to diverge from the drilling site. The same depositional environment is suggested by a progressive upward decrease in proportion of gravel particles and a decrease in sedimentation rate from 13.7 cm/1000 years at 480–400 m to 5.5 cm/1000 years at 400–270 m.

During the time spanning the interval from 270 to 0 m, the paleobasin may have acquired contours similar to the present-day outline, and its both sides were separated from the drilling site by deep depressions, i.e., the depositional environment was similar to the present-day environment. However, the lithological difference between the layers 270–110 m and 110–0 m must be due to climate changes.

Proceeding from the inferred changes in depositional environments and the age estimates of the lithologic

units of the BDP-98 section and using the paleotectonic reconstructions by Zonenshain, Kaz'min, and Moore [5, 7, 8], we may suggest a general evolution model for the study region spanning the last 11 Ma.

According to seismic data [8] and age estimates, seismoacoustic sequence B may have started to accumulate on the Akademichesky Ridge in the early Upper Miocene. At that time, the South and North depressions already existed as water basins, but the Akademichesky Ridge was still a land [8]. Our data indicate the existence of a broad basin about 10 Ma ago, which deepened toward the present-day western side of the lake. The drilling site is located on the eastern side of this basin; the Paleo-Barguzin delta was southwest of it, as shown by the seismic profile (Fig. 18). The load brought by the river formed the sediment fill at the drilling site as long as the early Upper Miocene (8.8 Ma ago).

In the Upper Miocene, the basin deepened and broadened, and the Akademichesky Ridge formed as an uplift dividing the North and Central basins. Deposition during the time span from 8.8 to 6.5 Ma ago was controlled by the river influx, namely, the supply of sediment load from the Paleo-Barguzin delta located north of the Ushkan'yi Isles [7]. Since the end of the Miocene (6.5 Ma ago), the deposition on the Akademichesky Ridge was free from the fluvial control and became purely pelagic.

Thus, there are three main stages in the formation of sediment section at the drilling site. The first included deposition on the slope or at the base of a limnic basin side. During the second, transitional, stage, the deposition at the base of a basin side graded into deposition on the top of a submerged uplift separated by deep depressions from the lake sides. The final stage was associated with deposition in the environment of a submerged uplift.

Within the limits of this model, the presence of turbidite layers at depths of 52 and 250 m needs additional explanation. Their existence on the top of an underwater ridge appears strange, as turbidite flows are, as a rule, broadly distributed in deep depressions [29]. The explanation may be as follows: The drilling site is bathymetrically below the ridge crest, and the slope is 1.5°. This is sufficient [30] for sediments — turbidites in this case — to slide downhill under seismic effects. Low thicknesses and scarcity of the turbidites indicates that seismic sliding played a minor role during the deposition of the upper section.

Climate control of deposition

Relative variations in the amount of diatom frustules are related to alternation of warm and cold climates in response to the Earth's orbital forcing [1, 4] and are traceable in the BDP-98 section as deep as the bore face. Thus, the climate change related to the astronomic factors occurred during the deposition of the section, i.e., from the early Upper Miocene (10.2 Ma ago). However, the amplitudes of these fluctuations in the Miocene were lower than later, possibly because of a smaller difference between the cold and warm periods. The warm subtropical climate of the Miocene in which conifer tree species were broadly distributed (exotic pines, spruce, tsuga [11]) may have been responsible for the appearance of amber-like rocks in the lower section.

As we wrote above, the conditions and rates of sedimentation vary throughout the section, which does not allow us to estimate the vertical climate variations without special studies, including palynology. At the same time, comparative paleoclimatic interpretation is possible in the upper 270 m section deposited under steady conditions. The sediments in the interval of 270 to 110 m contain abundant diatom frustules, which is evidence of a warmer climate favorable for diatom production. The formation of their silicic skeletons is provided by the presence of dissolved silica supplied by rivers. However, according to palynologic evidence, January temperatures were below zero in the late Miocene-early Pliocene and as low as –10 °C in the Early Pliocene [11]. The increase in the amount of sand lenses from the core depth of 250 m is related to transport of the sand-silt material by seasonal ice.

A drastic cooling 2.8–2.5 Ma ago is marked in many regions of the Northern Hemisphere [25]: In Europe, it was the earliest Pretiglian glaciating [30]; in North America, traces of glaciation are found as well [31]. In Siberia, there is no evidence of glaciation within this time span, though many authors suggest a quite severe cooling [12, 32].

The appearance of diatom-free fine clays in the Baikal section, similar to Late Pleistocene glacial clays, may attest to the presence of glaciers in the mountainous surroundings of Baikal as early as 2.8–2.5 Ma ago, because the mountains may have reached the altitudes sufficient for the formation of glaciers on their tops. The lobes of these glaciers may have reached the shoreline and deposit glacial pebbles (Fig. 6, *b*).

Another sharp cooling occurred 1.8–1.5 Ma ago, when glaciation embraced many regions of the Northern Hemisphere [12, 25, 30, 31]. Signs of a strong cooling, and even glaciation, are encountered in West Siberia and Prebaikalia as well [12, 31, 32]. Since 1.8–1.5 Ma ago, the behavior of climate in response to orbital forcing recorded in the Baikal sediments has held the same, which we studied earlier in detail [26].

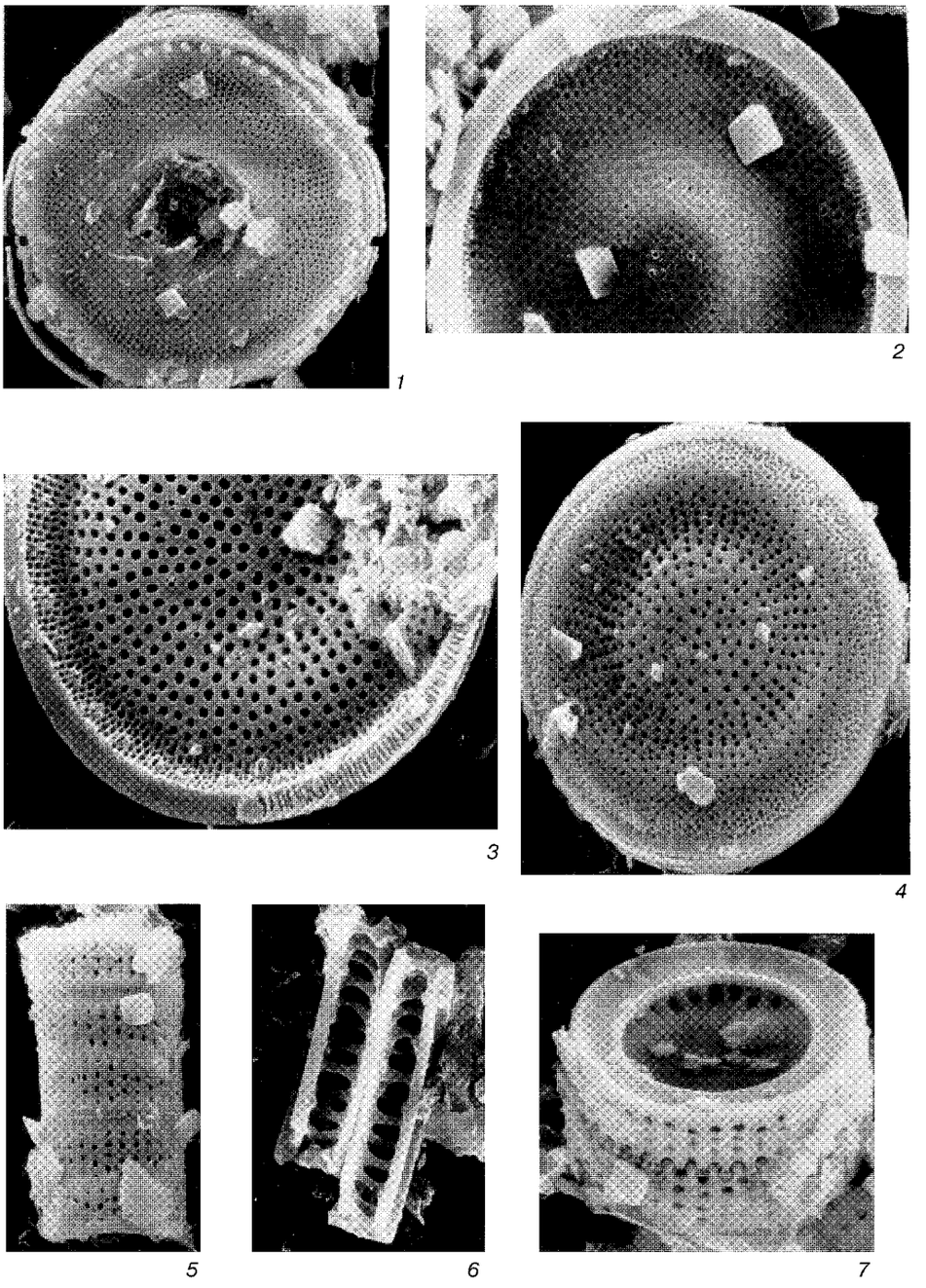

Fig. 19. Predominant genera of diatoms from of depths 500–600 m. *1*, *2* — *Concentrodiscus kuzminii* Khurs. & Fedenya sp. nov.; *3*, *4* — *Concentrodiscus* sp.; *5–7* — *Alveolophokjouseana* (Moiss) Moiss. Scale: *1*, *5* — 10 μm, *2–4*, *6*, *7* — 1 μm.

Preliminary investigation of the species composition of diatoms showed that the upper 200–220 m section contains diatom frustules similar to those discovered earlier in the BDP-96 core [34–36]. The lower part of the BDP-98 section contains frustules of diatoms found for the first time in the Baikal sediments (Fig. 19). At depths of 500–600 m, we discovered two new genera of diatoms. The genus *Concentrodiscus* Khurs., Moiss. et

Sukhova was first described in Miocene deposits of the Upper Syul'ban basin in Transbaikalia [37] and is extinct. In the Baikal bottom sediments we studied, this genus is represented by two new species: *Concentrodiscus kuzminii* Khurs. & Fedenya sp. nov. and *Concentrodiscus* sp. (Fig. 19). The genus *Alveolophoka* Moiss. et Neoretd. [38] is represented in the BDP-98 core by the extinct species *A. jouseana* (Moiss.) Moiss., which was broadly distributed in the Miocene in different regions of the Northern Hemisphere (Kamchatka, Far East, Transbaikalia, Belarus', and the western USA). The extinct diatom genera are important markers of Miocene deposits and can be used both for stratigraphic purposes and for remote correlations.

Distribution of vivianite nodules and sideritic rocks and their relation to climate change require further studies. Their unambiguous association with certain intervals of the section is, in our view, evidence for an origin under a climate control. Under the present-day conditions, an increase in water temperature may lead to deposition of carbonates, even if assuming the same water chemistry. The disappearance of carbonates in cold climates confirms this hypothesis.

Preliminary calculations using an earlier physicochemical equilibrium model of the Baikal water [39, 40] proved valid the hypothesis that carbonates may form in it. The boundary constraints are temperatures of 28–30 °C and a perfect equilibrium with the atmosphere.

Studies of interaction of the present-day Baikal water with the bottom sediments at high and low temperatures have shown that at high temperatures, carbonate precipitation is more intense, and the relative content of siderite, magnesite, and rodochrosite increases, though the general tendencies remain in action, such as authigenic formation of hydroxyl apatite, pyrite, and carbonates by diagenesis. Further lithological studies of carbonates will provide more details of their formation in the bottom sediments of Lake Baikal.

As a result of drilling of the BDP-98 borehole, a continuous 600 m thick sedimentary core, spanning 10.3 Ma, was obtained. The results of its studies bring more details into the paleoclimate record for Central Asia and may provide a basis for further higher-resolution reconstruction of the Upper Miocene-Holocene climate. Data of seismic stratigraphy and lithology obtained by drilling were correlated by acoustic logging, which made it possible to refine the geological history of the Baikal basin.

This work, as part of the Baikal Drilling Project, was supported by grants 97-05-9614, 97-05-96528, 97-05-96386, 97-05-96383, and 97-05-65340 from the Russian Foundation for Basic Research and grants EAR-94-13957 and EAR-96-14770 from US NSF. More support came from the Science and Technology Agency of Japan, Russian Ministry of Science, and Siberian Branch of the Russian Academy of Sciences. We thank all these institutions, especially the Russian Ministry of Science and Technology, for their concern and overall support of the project. Special thanks go to the crew of the BDP support ship *Baikal*, who piloted the drilling complex through the Baikal ice, and to the team of the Nedra Drilling Enterprise, who expertly completed the drilling program, as well as to people from the Institute of Geochemistry (Irkutsk) involved with the logistic support.

The publication was prepared by M. I. Kuz'min and E. B. Karabanov. The assistance of S. Kotomanova in preparation of the manuscript is especially appreciated.

REFERENCES

[1] The Baikal Drilling Project Group, *A continuous record of climate changes for the last five million years from the bottom sediments of Lake Baikal*, Geologiya i Geofizika (Russian Geology and Geophysics), vol. 39, no. 2, p. 139(135), 1998.

[2] BDP-93 Working Group, *Preliminary results of the first drilling on Lake Baikal, Buguldeika isthmus*, Geologiya i Geofizika (Russian Geology and Geophysics), vol. 36, no. 2, p. 3(1), 1995.

[3] M. I. Kuz'min, G. V. Kalmychkov, G. F. Geletii, et al., *Dokl. RAN*, vol. 362, no. 4, p. 541, 1998.

[4] D. F. Williams, J. A. Peck, E. B. Karabanov, et al., *Science*, vol. 278, p. 1114, 1997.

[5] L. P. Zonenshain, M. I. Kuz'min, V. G. Kaz'min, et al., *Dokl. RAN*, vol. 330, no. 1, p. 84, 1993.

[6] D. R. Hutchinson, A. J. Golmstok, L. P. Zonenshain, et al., *Geology*, vol. 20, p. 589, 1992.

[7] V. G. Kaz'min. A. Ya. Gol'mstok, K. Klitgord, et al., *Structure and development of the Akademichesky Ridge area (Baikal Rift) according to seismic investigations*, Geologiya i Geofizika (Russian Geology and Geophysics), vol. 36, no. 10, p. 164(155), 1995.

[8] T. C. Moore, K. D. Klitgord, A. J. Golmshtok, and E. Weber, *Geol. Soc. Amer. Bull.*, vol. 109, p. 746, 1997.

[9] V. D. Mats, A. G. Pokatilov, S. M. Popova, et al., *The Pliocene and Pleistocene history of Central Baikal* [in Russian], Novosibirsk, 1982.

[10] V. D. Mats, *Earth Sci. Rev.*, vol. 34, p. 81, 1993.

[11] V. A. Belova, *Late Cenozoic vegetation and climate of southern East Siberia* [in Russian], Novosibirsk, 1988.

[12] G. A. Vorobieva, V. D. Mats, and M. K. Shimaraeva, *Late Cenozoic paleoclimates in the Baikal region*, Geologiya i Geofizika (Russian Geology and Geophysics), vol. 36, no. 8, p. 82(80), 1995.

[13] E. B. Karabanov, A. A. Prokopenko, D. F. Williams, et al., *Quat. Res.*, vol. 50, p. 1, 1998.

[14] S. N. Chernyshov, *Fractures in rocks* [in Russian], Moscow, 1983.

[15] G. Mandl, *Mechanism of tectonic faulting. Models and basic concepts*, Amsterdam, 1988.

[16] K. Zh. Seminskii, *Principles and steps of special fracture-based mapping of a fault-block structure*, Geologiya i Geofizika (Russian Geology and Geophysics), vol. 35, no. 9, p. 112(94), 1994.

[17] I. M. Kutasov, *Geothermics*, vol. 16, nos. 5/6, p. 467, 1987.

[18] R. Von Herzen and A. E. Maxwell, *J. Geophys. Res.*, vol. 64, no. B10, p. 1557, 1959.

[19] J. W. King, J. A. Peck, P. Gangemi, and V. A. Kravchinsky, *Paleomagnetic and rock-magnetic studies of Lake Baikal sediments*, Geologiya i Geofizika (Russian Geology and Geophysics), vol. 34, nos. 10/11, p. 174(148), 1993.

[20] J. A. Peck, J. W. King, S. M. Colman, and V. A. Kravchinsky, *Earth Planet. Sci. Lett.*, vol. 122, p. 221, 1994.

[21] J. A. Peck, J. W. King, S. M. Colman, and V. A. Kravchinsky, *J. Geophys. Res.*, vol. 110, p. 11365, 1996.

[22] N. J. Shackleton, A. Berger, and W. R. Peltier, *Trans. Royal Soc. of Edinburgh: Earth Science*, vol. 81, p. 251, 1990.

[23] S. C. Cande and D. V. Kent, *J. Geophys. Res.*, vol. 100, no. B4, p. 6093, 1995.

[24] *Proc. Baikal Drilling Meeting, New Orleans, USA, 5 November 1995*, New Orleans, p. 39, 1995.

[25] N. A. Logatchev, I. V. Antoshchenko-Olenev, D. B. Bazarov, et al., *Uplands in Prebaikalia and Transbaikalia* [in Russian], Moscow, 1974.

[26] E. B. Karabanov, M. I. Kuz'min, A. A. Prokopenko, et al., *Dokl. RAN*, vol. 370, no. 1, p. 2000.

[27] T. G. Potemkina and V. A. Fialkov, *Geografiya i Prirodnye Resursy*, no. 2, p. 70, 1998.

[28] T. G. Potemkina, *Geografiya i Prirodnye Resursy*, no. 3, p. 50, 1998.

[29] M. I. Kuz'min, E. B. Karabanov, A. A. Prokopenko, et al., in: *Active tectonic continental basins*, Amsterdam, 2000.

[30] A. P. Lisitsyn, *Processes of terrigenous sedimentation in seas and oceans* [in Russian], Moscow, 1991.

[31] W. H. Zagwijn, in: *The dawn of the Quaternary. INQUA-SEQS-96*, Amsterdam, p. 2, 1996.

[32] K. V. Nikiforova, *Bull. Commission for Quaternary Studies*, no. 58, p. 37, 1989.

[33] V. S. Volkova and Yu. P. Baranova, *Pliocene and Early Pleistocene climatic changes in Northern Asia*, Geologiya i Geofizika (Soviet Geology and Geophysics), vol. 21, no. 7, p. 43(37), 1980.

[34] G. K. Khursevich, E. B. Karabanov, A. A. Prokopenko, et al., *IPPCCE Newsletter*, no. 12, p. 62, 1999.

[35] G. K. Khursevich, E. B. Karabanov, A. A. Prokopenko, et al., *ibid.*, p. 77.

[36] G. K. Khursevich, E. B. Karabanov, D. F. Williams, et al., in: *Proc. BICER, BDP and DIWPA Joint Intern. Symp. on Lake Baikal*, Yokohama, 2000.

[37] G. K. Khursevich, A. I. Moiseeva, and G. A. Sukhova, *Botanicheskii Zhurnal*, vol. 74, no. 11, p. 1660, 1989.

[38] A. I. Moiseeva and T. L. Nevretdinova, *Botanicheskii Zhurnal*, vol. 75, no. 4, p. 539, 1990.

[39] I. K. Karpov, K. V. Chudnenko, V. A. Bychinskii, and S. A. Kashik, *Dokl. RAN*, vol. 346, no. 3, p. 383, 1996.

[40] S. A. Kashik, I. K. Karpov, I. S. Lomonosov, and V. N. Mazilov, *Dokl. RAN*, vol. 335, no. 3, p. 359, 1993.

Recommended by G. N. Anoshin Received 17 May 1999